

**FINAL TECHNICAL REPORT**  
**ON**  
**SONOGELS IN THE PREPARATION OF ADVANCED GLASS AND**  
**CERAMIC MATERIALS**

**(Grant n° AFOSR-89-0533 A)**  
**for the period September 1, 1989-August 31 , 1992)**

**Submitted to AIR FORCE OFFICE OF SCIENTIFIC RESEARCH**

**by Professor J.ZARZYCKI**  
**Principal Investigator**

**Laboratory of Science of Vitreous Materials**  
**University of Montpellier II ; France**

document has been approved  
for release and sale to the public

**FINAL TECHNICAL REPORT**  
**ON**  
**SONOGELS IN THE PREPARATION OF ADVANCED GLASS AND**  
**CERAMIC MATERIALS**

**(Grant n° AFOSR-89-0533 A)**  
**for the period September 1, 1989-August 31 , 1992)**

**Submitted to AIR FORCE OFFICE OF SCIENTIFIC RESEARCH**

**by Professor J.ZARZYCKI**  
**Principal Investigator**

**Laboratory of Science of Vitreous Materials**  
**University of Montpellier II ; France**

|                    |  |
|--------------------|--|
| Accession For      |  |
| NTIS CR&I          | <input checked="checked" type="checkbox"/> |
| DTIC TAB           | <input type="checkbox"/>                   |
| Unannounced        | <input type="checkbox"/>                   |
| Justification      |  |
| By                 |  |
| Distribution /     |  |
| Availability Codes |  |
| Dist               | Avail and/or Special                       |
| A-1                |  |

**DTIC QUALITY INSPECTED 1**

## REPORT DOCUMENTATION PAGE

Form Approved  
OMB No. 0704-0188

|  |   |   |   |                          |                            |
|--|---|---|---|--------------------------|----------------------------|
| REPORT SECURITY CLASSIFICATION<br><b>UNCLASSIFIED</b>  |   |   | 1b. RESTRICTIVE MARKINGS  |                          |                            |
| SECURITY CLASSIFICATION AUTHORITY  |   |   | 3. DISTRIBUTION/AVAILABILITY OF REPORT<br>Approved for Public Release,<br>Distribution Unlimited. |                          |                            |
| DECLASSIFICATION/DOWNGRADING SCHEDULE  |   |   | 5. MONITORING ORGANIZATION REPORT NUMBER(S)   |                          |                            |
| PERFORMING ORGANIZATION REPORT NUMBER(S)   |   |   | 7a. NAME OF MONITORING ORGANIZATION<br>European Office of Aerospace Research<br>and Development.  |                          |                            |
| NAME OF PERFORMING ORGANIZATION<br>Université des Sciences et<br>Techniques du Languedoc   |   | 6b. OFFICE SYMBOL<br>(If applicable)                | 7b. ADDRESS (City, State, and ZIP Code)<br>Box 14<br>FPO NY 09510-0200                            |                          |                            |
| ADDRESS (City, State, and ZIP Code)<br>Place Eugène Bataillon<br>MONTPELLIER 34095 Cédex 05, FRANCE  |   | 8b. OFFICE SYMBOL<br>(If applicable)<br>NC          | 9. PROCUREMENT INSTRUMENT IDENTIFICATION NUMBER<br>AFOSR-89-0533                                  |                          |                            |
| NAME OF FUNDING/SPONSORING<br>ORGANIZATION AIR FORCE OFFICE<br>OF SCIENTIFIC RESEARCH  |   | 10. SOURCE OF FUNDING NUMBERS                       |   |                          |                            |
| ADDRESS (City, State, and ZIP Code)<br>Bolling AFB, DC 20332-6448  |   | PROGRAM<br>ELEMENT NO.<br>61102F                    | PROJECT<br>NO.<br>2303  | TASK<br>NO.<br>A3        | WORK UNIT<br>ACCESSION NO. |
| TITLE (Include Security Classification)<br><br>SONOGELS IN THE PREPARATION OF ADVANCED GLASS AND CERAMICS  |   |   |   |                          |                            |
| PERSONAL AUTHOR(S)<br>J. Zaccucchi   |   |   |   |                          |                            |
| 3a. TYPE OF REPORT<br>FINAL  | 13b. TIME COVERED<br>FROM 89/9/1 TO 92/8/31 | 14. DATE OF REPORT (Year, Month, Day)<br>1992/10/20 |   | 15. PAGE COUNT<br>116    |                            |
| SUPPLEMENTARY NOTATION   |   |   |   |                          |                            |
| COSATI CODES   |   |   | 18. SUBJECT TERMS (Continue on reverse if necessary and identify by block number)                 |                          |                            |
| FIELD  | GROUP                                       | SUB-GROUP   | GELS-ULTRASONICS-ULTRASTRUCTURE-CERAMICS-COMPOSITES.  |                          |                            |
|  |   |   |   |                          |                            |
| ABSTRACT (Continue on reverse if necessary and identify by block number)<br><br>I- Ceramic-ceramic composites for mechanical applications<br><br>Ultrasonic irradiation of mixtures of alkoxides and water (the sonocatalytic method) was shown to provide an interesting way of preparing matrices for ceramic-ceramic composites. The gelation speed of the "sonogels" can be sufficiently controlled to avoid the segregation of short $Al_2O_3$ or $ZrO_2$ fibres used as fillers. High homogeneity dispersions were produced in this way and the density of samples increased. In the case of cordierite, $5 SiO_2, Al_2O_3, 2MgO$ matrices the strength of the composite strongly depends on the type of crystallographic phase, $\mu$ -cordierite which is converted into $\alpha$ -cordierite by a thermal treatment. Hot-pressing proved necessary, however, to obtain samples with sufficient mechanical strength. A substantial increase in the resistance was obtained by the addition of optimal quantity of $TiO_2$ nucleant in precursor form to the starting cordierite sonosol. This method enables the hot-pressing to be performed while the matrix is in a glassy form, which improves the .../. |   |   |   |                          |                            |
| 20. DISTRIBUTION/AVAILABILITY OF ABSTRACT<br><input checked="" type="checkbox"/> UNCLASSIFIED/UNLIMITED <input type="checkbox"/> SAME AS RPT. <input type="checkbox"/> DTIC USERS  |   |   | 21. ABSTRACT SECURITY CLASSIFICATION<br>UNCLASSIFIED  |                          |                            |
| a. NAME OF RESPONSIBLE INDIVIDUAL<br>THOMAS E. ERSFELD, Capt, USAF   |   |   | 22b. TELEPHONE (Include Area Code)<br>(202) 767-4963  | 22c. OFFICE SYMBOL<br>NC |                            |

Abstract (continued):

compaction by viscous flow. A subsequent thermal treatment is used to convert the "seeded" glass matrix into fine-grain glass-ceramic. The mechanical strength depended on the volume fraction of the filler phase (fibres). The best results obtained were : 105 MPa for cordierite-ZrO<sub>2</sub> fibers and 158 MPa for cordierite-Al<sub>2</sub>O<sub>3</sub> fibers composites.

Especially interesting results were obtained infiltrating ZrO<sub>2</sub> ceramic felts by a cordierite "sonosol" and subsequent hot-pressing of multiple layered samples. The maximal mechanical strength obtained was 139 Mpa for the specimens treated at 1250°C for 6 hours.

The samples showed a very uniform infiltration. Further strength improvements could be made by optimizing the interfacial bond between the two ceramic phases.

II- Gels containing CdS nanoparticles for optical (non linear) applications

The sonocatalytic process was shown to lead to gels with a fine and uniform porosity. The chemical reactions in the pores enabled CdS nanoparticles to be produced by a gas diffusion method. The particles were in the 5-10 nm range and were studied by a variety of physico-chemical methods (high-resolution-transmission electron microscopy (HRTEM), small angle X-ray scattering (SAXS) and Raman spectroscopy. The optical transmission spectra showed the characteristic blue shift as a function of particle size, as predicted by the theory. The optical quality of the samples was substantially improved by an infiltration method using a "sonosol" which sealed the superficial pores and thus ensured higher longevity and permitted easy polishing of the samples.

**Researchers involved in the project :**

**Postgraduate students :**

**Manuel Piñero de los Ríos**  
graduate from University of Cádiz , Spain  
preparing a doctorate thesis jointly at  
the University of Cádiz and University of  
Montpellier.

**Eduardo Blanco Ollero**  
graduate from University of Cádiz , Spain  
preparing a doctorate thesis at the  
University of Cádiz

**Postdoctoral researches :**

**Dr. Milagrosa Ramírez del Solar**  
graduate from University of Cádiz , Spain

**Dr. Nicolás de la Rosa Fox**  
graduate from University of Sevilla ,  
Spain.

**Dr. Mohamed Atik**  
graduate from University of Montpellier ,  
France

**Publications :** **CORDIERITE- $\text{Al}_2\text{O}_3$  and CORDIERITE- $\text{ZrO}_2$   
COMPOSITES OBTAINED BY SONOCATALYTIC  
METHODS**

**M. Piñero , M. Atik , J. Zarzycki**

*Presented at the VI International  
Workshop on Glasses and Ceramics from  
Gels , October 6-11 , 1991 , Seville ,  
SPAIN , Journal of Non-Cryst. Solids ,  
147/8 , pp. (--) , 1992.*

**PROCESSING OF  $\text{ZrO}_2$  REINFORCED CORDIERITE  
COMPOSITES BY INFILTRATION OF CERAMIC  
FELTS WITH SONOSOLS**

**M. Piñero , J. Zarzycki , (Submitted to  
Journal of Sol-Gel Science and Technology)**

1. INTRODUCTION.
2. REVIEW OF 1<sup>st</sup> AND 2<sup>nd</sup> ANNUAL REPORTS
  - 2.1. Objectives
  - 2.2. Experimental Results Obtained
    - 2.2.1. Ceramic-ceramic Composites
      - 2.2.1.1. *Experimental Procedures*
      - 2.2.1.2. *Mechanical Properties*
    - 2.2.2. Inorganic Composites for Optical Applications
      - 2.2.2.1. *Experimental procedure*
      - 2.2.2.2. *Optical Properties*
  - 2.3. Previous Conclusions
  - 2.4. Objectives to be Accomplished
3. SYNTHESIS OF NEW CERAMIC-CERAMIC COMPOSITES
  - 3.1. Matrix Preparation
  - 3.2. Composites Processing
    - 3.2.1. Dispersion of Fillers
    - 3.2.2. Infiltration of Ceramic Felts
      - 3.2.2.1. *Preparation of the Matrix*
      - 3.2.2.2. *Gelation of Preforms*
      - 3.3.2.3. *Drying*
      - 3.3.2.4. *Hot-Pressing*
4. MEASUREMENT OF PROPERTIES OF CORDIERITE-BASED COMPOSITES
  - 4.1. Structural Analysis
  - 4.2. Physical Properties
    - 4.2.1. Relative Density
      - 4.2.1.1. *Sintered Samples*
      - 4.2.1.2. *Hot-Pressed Samples*
      - 4.2.1.3. *HIPed Samples*
    - 4.2.2. Thermal Expansion
  - 4.3. Mechanical Properties
5. SYNTHESIS OF SILICA SONOGEL MATRICES FOR OPTICAL APPLICATIONS
  - 5.1. Optical and Physical Requirements
  - 5.2. Study of Chemical and Physical Parameters
  - 5.3. Experimental Procedure
  - 5.4. Thermal Stabilization
  - 5.5. Impregnation Procedure

- 5.5.1. Experimental Observations of the Impregnation Process.

## 6. CHARACTERIZATION OF $\text{SiO}_2$ -CdS DOPED GELS

### 6.1. Evolution of Physical Properties.

### 6.2. Structural Analysis

- 6.2.1. Thermal Evolution Study

- 6.2.2. Textural Features

- 6.2.3. Transmission Electronic Microscopy

- 6.2.4. SAXS Measurements

- 6.2.4.1. *Titchmarsh Transformation*

### 6.3. Optical Properties.

- 6.3.1. Raman Spectroscopy

- 6.3.2. Absorption Spectroscopy

- 6.3.2.1. *Efros and Efros Model*

## 7. INTERPRETATION AND FINAL EVALUATION OF RESULTS

### 7.1. Ceramic-Ceramic Composites

### 7.2. Inorganic Composites for Optical Applications

## 8. FINAL CONCLUSION

## BIBLIOGRAPHY

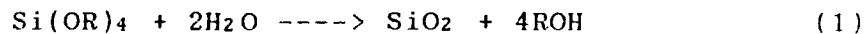
## INTRODUCTION



The sol-gel technology for preparing ultrahomogeneous glasses and ceramics constitutes an alternative route to the method of making glasses from oxide melts.

A significant part of sol-gel research is devoted to ceramic applications where high mechanical strength at elevated temperatures is required. Ceramic-ceramic composites are potentially interesting in this respect but the conventional techniques introduce a variety of problems of homogeneity and purity of final products which have hampered their development. These materials constitute an outstanding example of the need for applying more sophisticated chemistry to their processing.

The chemical reactions used in the sol-gel technology for preparing ceramics are illustrated by the hydrolysis of an alkoxysilane:



The hydrolysis reaction is generally obtained in the presence of a common alcoholic solvent for the alkoxide and water to prevent immiscibility phenomena.

Recent studies [1] based on the application of ultrasonic radiation to the sol-gel process have shown that high density "sonogels" which have a larger specific surface than those

observed for classical gels could be obtained by this method. The ultrasounds are applied during the hydrolysis of the precursor alkoxide thereby avoiding the use of a solvent. Moreover the ultrasonic dose constitutes an additional parameter to control the final texture of the gels.

The characteristics of sonogels should therefore constitute a substantial advantage for sintering at lower temperatures in comparison to materials obtained by classic sol-gel techniques applied to ceramic composite processing.

The sonocatalytic approach has recently been used for preparing composites of the  $\text{SiO}_2$ - $\text{SiO}_2$  system [2] introducing fine silica particles (Aerosil) into a  $\text{SiO}_2$  "sonosol".

In our research programme cordierite ( $5\text{SiO}_2$   $2\text{Al}_2\text{O}_3$   $2\text{MgO}$ ) was selected for preparing the ceramic matrix of the composites, because of the low coefficient of thermal expansion ( $10^{-6}$ - $10^{-7}$ ) and relatively high mechanical strength ( $\approx 200$  -  $300$  MPa) of this compound. We studied its fabrication by the sonogel route and investigated the effect of the addition of  $\text{TiO}_2$  on the nucleation and crystalization process.

The  $\text{SiO}_2$ - $\text{TiO}_2$  system which possesses a very low and linear expansion coefficient which can be close to zero, was also considered as an interesting possibility for use as a ceramic matrix in the processing of composites. Work reported elsewhere [3] has demonstrated the possibility of preparing homogeneous  $\text{SiO}_2$ - $\text{TiO}_2$  sonogels with 1-15 mol %  $\text{TiO}_2$ . Its conversion into an aerogel has also been reported [3].

To constitute ceramic-ceramic composites different reinforcing phases were used in the form of  $ZrO_2$  and  $Al_2O_3$  short fibres and of  $ZrO_2$  and  $Al_2O_3$  ceramic felts [4].

As shown by recent works [5] using SAXS measurements on  $SiO_2$  sonogels, they possess an extremely fine porosity, the size of pores being of the order of 20 Å. This has suggested their use as matrices for preparing composites containing small-sized particles by chemical precipitation within the pores.

In the present work a method is proposed for preparing an small-sized CdS particles phase dispersed in a  $SiO_2$  stabilized sonogel host-matrix.

This work is motivated by recent experimental interest concerned with the optical properties of small (<100 Å) semiconductor microcrystals. The interest stems from the optical behaviour observed when the crystallite size becomes sufficiently small enough to restrict the allowable electronic energy levels. The quantum confinement effects lead to interesting application in the field of non-linear optics.

## 2. REVIEW OF 1<sup>st</sup> AND 2<sup>nd</sup> ANNUAL REPORTS

## 2.1. OBJECTIVES

The main objectives of this work were to evaluate experimentally the applicability of "sonogels" as precursor materials for two kinds of advanced composite materials:

- I. Ceramic-ceramic refractory composites with high mechanical strength
- II. Inorganic composites for non-linear optical applications.

## 2.2. EXPERIMENTAL RESULTS OBTAINED

### 2.2.1. Ceramic-ceramic composites

#### 2.2.1.1. Experimental Procedures

Sonogels of two different types ,  $5\text{SiO}_2$   $2\text{Al}_2\text{O}_3$   $2\text{MgO}$  (cordierite) and  $(100-x)\text{SiO}_2 - x\text{TiO}_2$  (with  $x=1,5,10,15$  and  $20$ ) were prepared.

Tetraethoxysilane  $\text{Si}(\text{OEt})_4$  (TEOS) was used as silica source , aluminium sec-butoxide  $\text{Al}(\text{OBu}^s)_3$  (ASB) for alumina , magnesium acetate tetrahydrate  $\text{Mg}(\text{Ac})_2 \cdot 4\text{H}_2\text{O}$  for magnesia and tetrabutyl orthotitanate  $\text{Ti}(\text{OBu})_4$  (TBOT) for titania.

The hydrolysis reaction of different precursor alkoxides was achieved by submitting the alkoxides-water mixture to

ultrasonic irradiation with doses of 70 - 150 J/cm<sup>2</sup>. By this method the otherwise necessary presence of a common solvent for obtaining homogeneous gels was avoided.

Highly homogeneous ceramic-ceramic composites were obtained by mechanical dispersion of different reinforcing phases : ZrO<sub>2</sub> , Al<sub>2</sub>O<sub>3</sub> and SiC in the form of short fibres , in cordierite and silica-titania sonosols before gelation took place. Volume fraction of the reinforcing phase was 50-60 % in all cases.

The samples were dried by simple heat-treatment schedule using different soaking times and temperatures ( cf. previous work).

Devitrification of cordierite samples was controlled by adding 1,7 or 11 wt % TiO<sub>2</sub> to the starting sonosol in the precursor form (TBOT). The heat treatment schedule for devitrification was designed from differential thermoanalysis studies combined with X-ray diffraction analysis.

Dried samples were densified in the monolithic form by sintering up to 1400 °C for 24 hours.

Relative densities of samples after sintering varied from 50 % for SiO<sub>2</sub>-TiO<sub>2</sub> - based composites to 80-85 % for composites involving cordierite.

These low relative densities were caused by non-desired crystallization effects in respective matrices during the

sintering process and which could be substantially increased only in the case of the cordierite samples using hot-pressing techniques.

The  $\text{SiO}_2\text{-TiO}_2$  sonogels crystallized at low temperatures ( $\sim 700^\circ\text{C}$ ) impeding densification even when hot-pressing was used because of the high viscosity of the glass developed in this system.

The best conditions of densification for cordierite-based composites were:

- 20-40bar pressure
- 15-60 minutes soaking temperatures between  $700\text{-}1000^\circ\text{C}$ .

Fully densified cordierite glasses were obtained using hot-pressing for 20 min. at  $900^\circ\text{C}$  with 20 bar pressure with relative densities up to 99% .

Devitrification was found for samples treated at  $950^\circ\text{C}$  in the form of  $\mu$ -cordierite , a metastable form which transforms to the high temperature  $\alpha$ -cordierite , a form stable at  $1000\text{-}1050^\circ\text{C}$  and which is present up to the melting point ( $1465^\circ\text{C}$ ).

Devitrification of cordierite was found at lower temperatures ( $900^\circ\text{C}$ ) when 11 %  $\text{TiO}_2$  was present.

### 2.2.1.2. Mechanical Properties

The mechanical strength of the cordierite matrix was measured by the three-point bending test ; the highest value (~100 MPa) was obtained for compositions containing 11 wt %  $\text{TiO}_2$  with  $\mu$ -cordierite form densified at 950°C.

This value dropped to ~ 40 MPa when  $\alpha$ -cordierite was the structural major form for a composition with 7 wt %  $\text{TiO}_2$  , the sample being heat treated for 2 hours at 1150 °C.

Hot-pressed composites showed the same temperature dependence behaviour that the isolated matrix. The highest strengths (105 MPa) were obtained for a  $\mu$ -cordierite /(  $\text{ZrO}_2$  64 % vol) composite and 160 MPa for a  $\mu$ -cordierite( $\text{TiO}_2$  7% wt)/( $\text{Al}_2\text{O}_3$  50 % vol) composite . The maximal strengths obtained for the same compositions when the matrix was in the stabilized  $\alpha$ -form , following heat treatment , were 75 and 110 MPa respectively.

These values were higher than those for cordierite-based composites obtained by sintering monolithic cylindrical samples , where mechanical resistance was determined by means of the "brazilian" test [6] , and which gave 35-40 MPa as the maximal strength.



## 2.2.2. Inorganic composites for Optical Applications

### 2.2.2.1. Experimental Procedure

SiO<sub>2</sub> sonogels were prepared from TEOS with a molar ratio 1:4:4 of TEOS:water:formamide. A cadmium salt was added to the sonosolution in different quantities (1,5,8,10,15,20,25,30 and 40 mol % with respect to SiO<sub>2</sub>).

The ultrasonic dose applied was 200 Jcm<sup>-3</sup>.

In some cases drying chemical control additives (DCCA) other than dimethyl formamide (DMF) were used or the DCCA omitted.

For comparison a classic gels were prepared with the same compositions sonogels using EtOH 50 % vol /vol TEOS as common solvent.

Gelation , aging and drying were effected at 40 °C for different soaking times.

CdS nanoprecipitates were formed in the gels by exposure to SH<sub>2</sub> vapours at 40 °C. Particles of 5-15 nm diameter were observed by TEM for these sonogels samples

In order to obtain a physically stabilized silica-CdS sonogel , the samples were then superficially impregnated with a SiO<sub>2</sub> sonosol then gellified and dried again.

Finally the surfaces were polished to obtain optically transparent gel samples.

#### 2.2.2.2. Optical Properties

The optical absorption spectra of the different doped gels indicated the presence of a shoulder at 440 nm but they presented an insufficient optical density.

#### 2.3. PREVIOUS CONCLUSIONS

1. The sonocatalytic method provides an alternative way to conventional methods for preparing highly homogeneous ceramic-ceramic composites.
2. In  $\text{SiO}_2\text{-TiO}_2$  and cordierite systems successful sintering is prevented by non-desired crystallization effects
3. Hot-pressing constitutes an alternative route to avoid crystallization phenomena during sintering in the case of cordierite sonogels.
4. Cordierite-based composites present relatively low strength because of the formation of porosity in the matrix at temperatures higher than 1000 °C due to the  $\mu$ -cordierite to  $\alpha$ -cordierite transformation.
5. The addition of 7-11 wt % of  $\text{TiO}_2$  to cordierite sonogels brings about an increase of mechanical resistance of hot-pressed samples.

6. A fine dispersion of CdS particles can be developed in a SiO<sub>2</sub> sonogel matrix.

#### 2.4. OBJECTIVES TO ACCOMPLISH

The main objectives to be accomplished were :

1. Increase in the mechanical resistance for cordierite matrix and composites . This was attempted by increasing the amount of the nucleant agent in order to develop a higher concentration of TiO<sub>2</sub> nuclei uniformly dispersed in the matrix.

2. Preparation of new ceramic-ceramic composites by infiltration of the ceramic matrix , in the sonosol precursor form , into different ceramic felts.

3. Experimental evaluation of various precursors , and new compositions for obtaining SiO<sub>2</sub> gels with a narrow pore size distribution in order to obtain favorable conditions for a fine and homogeneous dispersion of CdS particles.

4. Improving of exposure procedure to SH<sub>2</sub> vapours in order to develop CdS-doped SiO<sub>2</sub> sonogels with higher optical density.

- 5.- Improving stability of SiO<sub>2</sub> matrix in order to prevent mechanical failure and optical transparency losses during aging.

### 3. SYNTHESIS OF IMPROVED CERAMIC-CERAMIC COMPOSITES FROM SONOGELS

New ceramic-ceramic composite materials were prepared by:

- increasing the amount of  $\text{TiO}_2$  nucleating agent in cordierite ceramics, from 7-11 wt % in our previous work, up to 15 wt %. The fillers were added in a volume fraction varying from 10 to 60 %, both for  $\text{ZrO}_2$  and  $\text{Al}_2\text{O}_3$  (Zircar Products) ceramic fibres.

- using other reinforcing phases in the form of  $\text{ZrO}_2$  (ZFY-100, Zircar Products) and  $\text{Al}_2\text{O}_3$  (MAFTEC) ceramic felts.

### 3.1. Matrix Preparation

The cordierite ceramic matrix was prepared as discussed in the 2<sup>nd</sup> Annual Report and schematized in Figure 1.

In the preparation of cordierite the following starting materials provided by FLUKA were used :

TEOS (Tetraethoxysilane), > 98 %,  $(\text{Si}(\text{OEt})_4)$ ,

ASB (Aluminum sec-butoxide), pract. 21 %  $\text{Al}_2\text{O}_3$ ,  $(\text{Al}(\text{O}i\text{Bu})_3)$

Magnesium acetate tetrahydrate, > 99 %,  $(\text{Ac}_2\text{Mg} \cdot 4\text{H}_2\text{O})$

The nucleating agent  $\text{TiO}_2$  (15 wt %) was added to the cordierite sonosol in the sol-precursor form of tetrabutyl

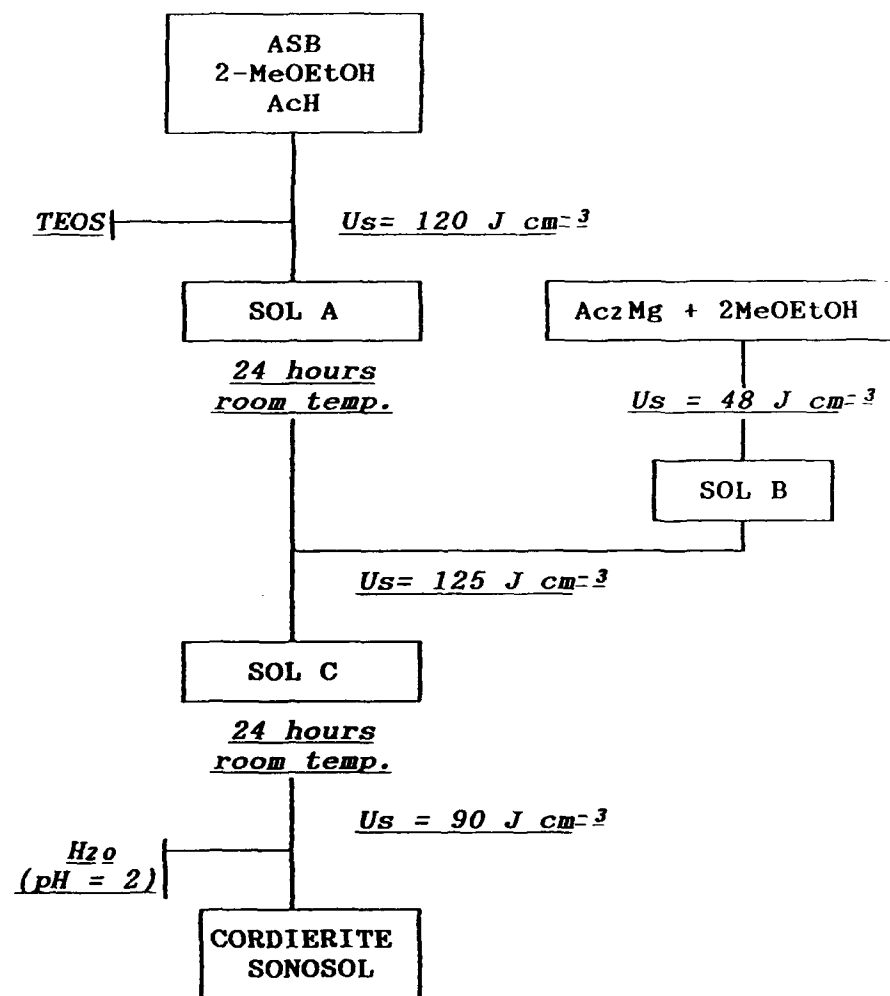


Figure 1. Schematic route for preparing cordierite sonogels

orthotitanate (TBOT) before hydrolysis , in order to achieve a fine-grained crystallization by internal nucleation.

It was observed that after hydrolysis reaction of solution C the time of gelation increased by 10-100 times , depending on the TiO<sub>2</sub> content , when the soaking time for C solution varied from 1 to 45 days. Table 1. shows the influence on t<sub>gel</sub>. of soaking time for C solution.

Table 1

| Soaking Time<br>of C-solution | TiO <sub>2</sub> (wt%) | t <sub>gel</sub>                 | T(°C) |
|-------------------------------|------------------------|----------------------------------|-------|
| 24 h                          | 0<br>7<br>11<br>15     | 30 m.<br>10 m.<br>2 m<br>in situ | 20    |
| 1 week                        | 0<br>7<br>11<br>15     | 1 h<br>15 m<br>10 m<br>5 m       | 20    |
| 1 month                       | 0<br>7<br>11<br>15     | 7 h<br>5 h<br>4 h<br>3 h         | 20    |

In the preparation of composites with high volume fractions of the reinforcing phase (>40 % ) and 11 - 15 wt % TiO<sub>2</sub> , we used c-sonosolutions 3 - 4 weeks aged in order to avoid a fast gelation induced by the temperature increase which occurs during the dispersion of fillers with a high rotatory blender (ULTRATURRAX).

Amorphous white powders with cordierite composition were obtained from dried sonogels. Drying was effected up to 700 °C both in the air and then in oxygen atmosphere to accomplish the total elimination of organic residues. The time-temperature program followed for drying-curing is shown in Figure 2.

Calcined powders were compacted in a mould with a force of 4-6 ton . Compact pellets of 13.2 mm diameter and 3-5 mm thickness were produced ready for sintering in an electric furnace.

Hot-pressing technique was used in order to achieve an increase in final relative densities after densification .The conditions for hot-pressing were 20-40 bar and 700 to 1000°C . These conditions were maintained for 15-60 minutes.

Final samples were obtained in a form of disks 26 mm in diameter and 2-4 mm thickness .

### 3.2. Processing of Composites

Two different methods were employed in the preparation of composites :

1. Dispersion of  $ZrO_2$  or  $Al_2O_3$  ceramic fibers (Zircar Products) into cordierite sonosols
2. Infiltration of the sonosol matrix into  $ZrO_2$  (ZYF-100 , Zircar Products) or  $Al_2O_3$  (MAFTEC) ceramic felts



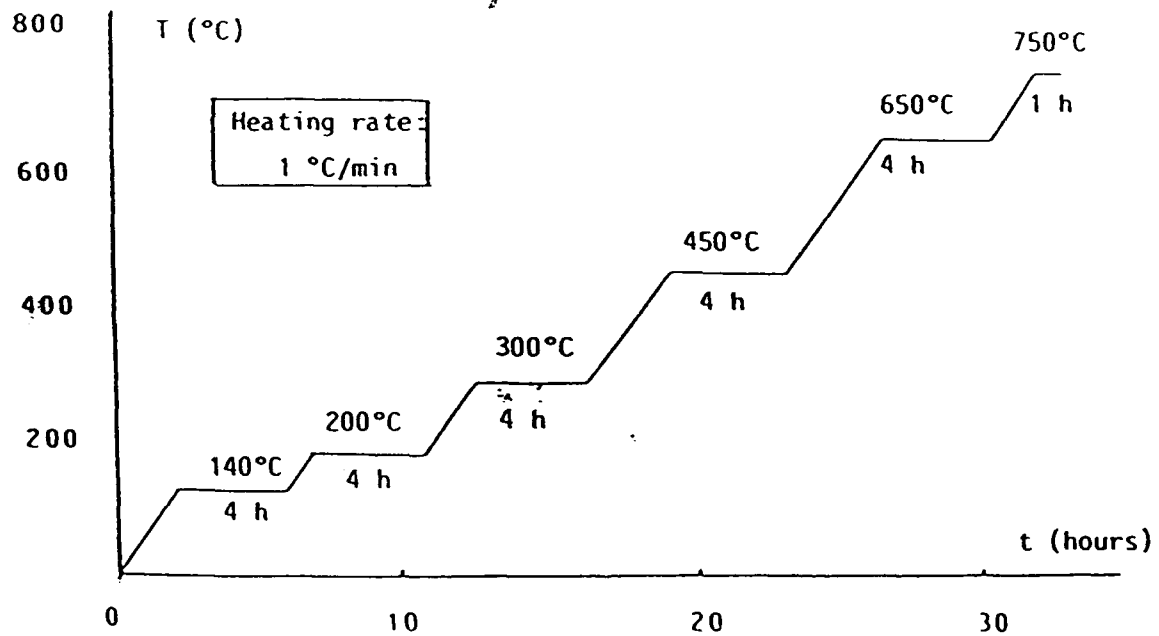


Figure 2. Sequence of steps followed for the elimination of organic residues of cordierite sonogels and composites.

### 3.2.1. Dispersion of the Fillers

As was reported in our previous work (1st and 2nd Annual technical report) , short fibres of ceramic compounds can be easily dispersed in a low viscosity matrix obtained by the sol-gel process.

Cordierite-based composites samples will be noted CZx , for cordierite/ZrO<sub>2</sub> , and CAy for cordierite/Al<sub>2</sub>O<sub>3</sub> composites , with x and y designing the volume fraction of ZrO<sub>2</sub> and Al<sub>2</sub>O<sub>3</sub> fillers.

In this part of the study we used a high speed rotatory blender (ULTRATURRAX TP18/10) at 20,000 rpm which ensures a high homogeneous dispersion of the fibres through the whole volume of the solution. At the same time , gelation of the matrix is accelerated by the effects induced by the action of high speed agitation.

The gelation time of the dispersed solution could be controlled by adjusting the following parameters :

- ultrasonic dose
- agitation dose
- TiO<sub>2</sub> wt %

Ultrasonic doses used were  $\approx 450$  Jcm<sup>-3</sup> and the agitation times employed varied from 3-10 minutes which were equivalent

to 180-600 Jcm<sup>-3</sup> for a volume of 45 cm<sup>3</sup> , while the temperature of the solution reached 85°C.

Gelation took place at 100°C and the time for this was 1-5 minutes.

Aging was effected at 50°C for 24 hours in closed containers.

Drying was carried out for 48 hours at 100°C . Then the specimens were heat-treated up to 700°C at a heating rate of 1°C/min in O<sub>2</sub> atmosphere , maintaining soaking times at critical temperatures.(See Figure 2.)

Final densification was achieved by sintering at 1400°C for 4 1/2 hours for CZx composites ,( for higher soaking times the matrix flowed with deformation of the whole sample) , or by hot-pressing at 900-1000°C and 20-40 bar for 20-30 minutes.

Sintering of CAx composites gave low relative densities even for soaking times higher than 30 hours. However , densification by hot-pressing for the last composites was easily obtained in the same conditions as for CZx samples.

For the sake of comparison a cordierite glass obtained by direct melting from oxides provided by Corning Europe was used to prepare composites with the same reinforcing phases.

For this , 100 g. of cordierite glass was mechanically ground for 6 hours in different crushing-machines , obtaining a fine powder.

Samples were prepared by solid mixing of 20 % vol. Al<sub>2</sub>O<sub>3</sub> or ZrO<sub>2</sub> with the glass powder and densification was achieved by hot-pressing in the same conditions as for sonogels.

These samples were very similar to those obtained by sol-gel techniques but presented a black colour after hot-pressing at 900°C (white for sonogels). This was attributed to the presence of contamination by oxidized metallic particles from the glass-crushing devices.

Hot Isostatic Pressing (HIP) at 1400°C was also employed to complete sintering in CA<sub>x</sub> samples. Fully densified ceramic composites were obtained by this way.

### 3.2.2. Infiltration of Ceramic Felts

The method consisted of four steps:

1. Preparation of ceramic matrix solution
2. Preparation and gelation of the preform
3. Drying
4. Hot-pressing.

#### *3.2.2.1. Preparation of the Matrix*

The solution used was a cordierite sonosol with x wt % TiO<sub>2</sub>, (x = 0, 7, 15).

Long-aged (15 days) C-solutions were used for infiltrating ceramic felts which provided a most effective penetration of the matrix because of the low viscosity of the sol.

#### *3.3.2.2. Gelation of Preforms.*

The  $ZrO_2$  and  $Al_2O_3$  ceramic felts used were made from ceramic fibres. In both cases the fibres were largely continuous and randomly oriented in planes parallel to the layers.

The zirconia refractory felt was shaped in form of 2.5 mm thick layer with  $0.24 \text{ g cm}^{-3}$  bulk density. The alumina felt was 25 mm of thickness and  $0.096 - 0.128 \text{ g cm}^{-3}$  in density.

The felts were cut into required pieces (26 mm diameter and 2.5-4.0 mm thick) and placed in plastic containers filled with the sonosol. The organometallic sonosol had a very strong tendency to wet the zirconia or alumina felts and the impregnation process could be easily achieved under primary vacuum.

The samples were left in the solutions under primary vacuum during 1-2 hours. After this time they were placed in an oven at  $100^\circ\text{C}$  for 24 hours for gelation.

#### *3.3.2.3. Drying.*

After gelation the samples were heat treated in order to remove the water and residual organic matter. The sequence steps of thermal treatment for drying was determined from the TGA study of each sample ; as shown in Figure 3.

The volume fraction of the matrix introduced into the ceramic felts by the infiltration process was measured at this stage by weighing the samples and is shown in Table 8 for a number of consecutive infiltrations.

The volume fraction of the reinforcing phase was controlled by the number of infiltrations effected.

During the last infiltration, the preforms were superimposed, up to 4-6 preforms forming a layered structure.

#### *3.3.2.4. Hot-Pressing*

The layer preform was hot-pressed at 900-930°C temperature and 40 bar pressure. The maximum temperature was maintained at 20-30 minutes until densification was completed.

Densified samples of 26 mm diameter and 2-4 mm thickness were obtained.

#### 4. MEASUREMENT OF PROPERTIES FOR CORDIERITE-BASED COMPOSITES

#### 4.1. Structural Analysis

The weight losses of cordierite sonogels were determined by thermogravimetric analysis which gave the following temperature ranges :

- 100-160°C    evaporation of residual alcohol and water traces
- 220-300°C    oxidation of non-reacted organic groups or those introduced by reesterification.
- 430-480°C    condensation of residual -OH groups

These ranges were approximately the same for cordierite - titania samples.

From this analysis we proposed the thermal program for removing organic residues shown in Figure 2.

From differential thermoanalysis (DTA) combined with X-ray diffraction analysis the structural crystalline polymorphic forms of cordierite were determined as follows:

- $\mu$ -cordierite : metastable low-temperature form (850-950°C)
- $\alpha$ -cordierite : stable high-temperature form (950-1465°C)

The formation of  $\mu$ -cordierite was observed at 950°C for samples prepared without the addition of titania and at 900°C for samples with 7 wt % titania .



This effect was attributed to the nucleating action of titania which favored the crystallization process.

## 4.2. Physical Properties

### 4.2.1. Relative Density

#### 4.2.1.1. Sintered Samples

Relative densities ,  $D_r$  , of the cordierite ( $\text{TiO}_2$  15 wt %) matrix and composites were measured by Archimedes' principle in water. Table 2 shows the relative densities and the porosity ,  $\pi_o$  , experimentally obtained after sintering for different samples which were compressed from calcined powders under experimental conditions described in § 3.1.

These values range from 60 % of theoretical density  $d_{th}$  for a CA<sub>50</sub> composite sintered at 1300°C for 12 hours , to 98 %  $d_{th}$  for a CZ<sub>55</sub> composite sintered at 950°C during 2 hours and then at 1400 °C for 4 1/2 hours.

Cordierite samples containing  $\text{TiO}_2$  in 0,7,11 and 15 wt % , designated Co , CT7 , CT11 and CT15 , were sintered at temperatures ranging from 950 °C to 1400°C for 4-24 hours.

The minimal and maximal relative densities obtained for these samples were 68 % at 950°C , 15 hours for CT11 and 900°C , 2 hours then 1300°C , 5 hours for CT15.

It was also observed that cordierite samples deformed by viscous flow starting from 1400°C.

Table 2

Physical properties for sintered cordierite-based glass and ceramics obtained by sol-gel process.

| Sample | Dr<br>(%) | $n_o$<br>(%) | Sintering           |              |
|--------|-----------|--------------|---------------------|--------------|
|        |           |              | T(°C)               | t(h)         |
| Co     | 85        | 8            | 1000                | 24           |
| CT7    | 80        | 5            | 950<br>1400         | 24<br>24     |
| CT11   | 68        | 36           | 950                 | 15           |
| CT15   | 86        | 7            | 900<br>1300         | 2<br>4       |
| CT15   | 90        | 12           | 900<br>1300         | 2<br>5       |
| CZ50   | 98        | -            | 950<br>1400         | 2<br>9       |
| CZ55   | 98        | -            | 950<br>1400         | 2<br>4 1/2   |
| CZ50   | 77        | 40           | 950<br>1300<br>1400 | 2<br>15<br>9 |
| CA60   | 65        | 42           | 950<br>1400         | 2<br>4 1/2   |
| CA50   | 60        | 45           | 1300                | 12           |

-As crystallization of cordierite occurs between 900-950°C where  $\mu$ -cordierite is developed and the transformation to  $\alpha$ -cordierite at 1000-1050°C, accompanied by an increase in total volume of specimen, it follows that the viscous sintering is hindered by the first crystallization at 950°C.

Increasing the temperature to 1000°C produces a decrease in viscosity which facilitates the flow of the matrix containing the crystals formed.

The transformation to  $\alpha$ -cordierite at 1000°C results in the formation of a residual porosity which prevents total densification.

It can be observed in Table 2 that these conclusions are in accordance with the experimental results obtained for relative densities.

In the case of composites the presence of fillers constituted an additional problem for sintering because they obstruct the matrix flow.

#### *4.2.1.2. Hot-pressed Samples*

##### *I. Composites obtained by dispersion of fillers in cordierite sonosols*

Hot-pressing of composites allowed relative densities of 99 % to be obtained. The conditions for sintering were 20-40 bar with temperature ranging between 900°C and 1000°C.

From X-ray diffraction spectra of hot-pressed samples it was observed that at 900-925°C the cordierite matrix was obtained in a glassy form. When the temperature was increased to 950°C, the matrix crystallized in the  $\mu$ -cordierite metastable form. The high temperature stable form,  $\alpha$ -cordierite, was obtained above 1000°C.

Relative densities,  $D_r$ , and porosity,  $w_0$ , for hot-pressed samples, Co, CT7, CT11 and CT15 matrices, heat-treated at different temperatures are shown in Table 3.  $D_r$  values were around 99 % both for the non-devitrified glass or the crystalline cordierite.

This indicates the substantial improvement obtained in the densification process, achieved by means of hot-pressing, compared to results obtained in conventional sintering.

Table 4 shows the relative densities obtained for hot-pressed composites with a CT15 matrix and ZrO<sub>2</sub> ceramic fibres as the reinforcing phase. They are designated as CT15Z<sub>x</sub> where  $x$  is the volume fraction of zirconia, the  $g$ ,  $\mu$ , or  $\alpha$  index designating the glass or the crystalline forms of the matrix.

Table 5 gives the relative densities for the CT15 / Al<sub>2</sub>O<sub>3</sub> composites. They are designated as CT15A<sub>y</sub>, where  $y$  is the volume fraction of alumina ceramic fibres.

As a general conclusion for the densification stage achieved in these samples, it can be observed that:

Table 3

Physical and mechanical characteristics for a) hot-pressed cordierite b) cordierite/ZrO<sub>2</sub> composites and c) cordierite/Al<sub>2</sub>O<sub>3</sub> composites with different TiO<sub>2</sub> contents

Table 3a

| Sample | Dr (%) | n° (%) | Hot-pressing |          |           | Strength (MPa)               | Young's Modulus (GPa) |
|--------|--------|--------|--------------|----------|-----------|------------------------------|-----------------------|
|        |        |        | T (°C)       | P (bar)  | t (min)   |                              |                       |
| Co     | 97     | 4      | 1000         | 30       | 20        | 70                           | 23.40                 |
| CT7    | 98     | 3      | 1150         | 30       | 20        | 43.10                        | 16.45                 |
| CT11   | 99     | 2      | 950          | 30       | 15        | 96.70                        | 31.00                 |
| CT15   | 99     | 1      | 900          | 25       | 25        | 23                           | 7.15                  |
| CT15   | --     | --     | 900<br>1250  | 25<br>-- | 25<br>300 | failed during heat treatment |                       |

Table 3b

|                   |    |    |             |          |           |        |       |
|-------------------|----|----|-------------|----------|-----------|--------|-------|
| CoZ <sub>62</sub> | 90 | -- | 950         | 30       | 15        | 45     | 18.30 |
| CoZ <sub>64</sub> | 90 | -- | 980         | 40       | 60        | 105.20 | 30.90 |
| CoZ <sub>66</sub> | 90 | -- | 980<br>1050 | 40<br>-- | 60<br>120 | 74.70  | 23.00 |

Table 3c

|                    |    |    |              |          |           |        |       |
|--------------------|----|----|--------------|----------|-----------|--------|-------|
| CoA <sub>52</sub>  | 93 | -- | 950          | 30       | 15        | 38     | 9.70  |
| CoA <sub>49</sub>  | 99 | -- | 1000         | 30       | 15        | 110.50 | 31.50 |
| CoA <sub>48</sub>  | 95 | -- | 900<br>1150  | 40       | 60<br>120 | 96.30  | 29.70 |
| CT7A <sub>51</sub> | 95 | -- | 1000         | 40       | 20        | 158    | 41.25 |
| CT7A <sub>52</sub> | 92 | -- | 1000<br>1050 | 40<br>-- | 20<br>120 | 106    | 32.00 |

**Table 4**  
Physical and mechanical properties for hot-pressed  
cordierite(TiO<sub>2</sub> 15 % wt )/ ZrO<sub>2</sub> fibres - composites obtained  
from sonogels.

| Sample  | Dr<br>(%) | no<br>(%) | Hot-pressing |        |        |  | Strength (MPa) |         |  | Young's modulus<br>(GPa) |       |  | No. of<br>tests |
|---------|-----------|-----------|--------------|--------|--------|--|----------------|---------|--|--------------------------|-------|--|-----------------|
|         |           |           | T(°C)        | P(bar) | t(min) |  | Mean           | Range   |  | Mean                     | Range |  |                 |
| CT15Z60 | 92        | 26        | 920          | 25     | 30     |  | 82.42          | 73-91   |  | 23.76                    | 19-25 |  | 7               |
| CT15Z60 | 90        | 27        | 925          | 25     | 30     |  | 104.00         | 107-135 |  | 32.45                    | 11-43 |  | 7               |
|         |           |           | 1100         | --     | 180    |  |                |         |  |                          |       |  |                 |
| CT15Z50 | 93        | 21        | 920          | 25     | 25     |  | 87.00          | 64-106  |  | 29.72                    | 15-47 |  | 17              |
|         |           |           | 906          | 25     | 30     |  | 93.22          | 89-106  |  | 32.78                    | 24-40 |  | 5               |
| CT15Z50 | 92        | 22        | 920          | 25     | 30     |  | 91.68          | 68-115  |  | 28.62                    | 21-37 |  | 9               |
|         |           |           | 1200         | --     | 120    |  |                |         |  |                          |       |  |                 |
| CT15Z40 | 93        | 12        | 920          | 25     | 30     |  | 101.74         | 98-104  |  | 35.74                    | 35-36 |  | 2               |
| CT15Z30 | 96        | 2         | 925          | 25     | 20     |  | 106.10         | 98-113  |  | 42.58                    | 42-43 |  | 2               |
| CT15Z20 | 99        | 0.3       | 908          | 25     | 25     |  | 107.40         | 102-112 |  | 36.70                    | 35-38 |  | 2               |

**Table 5**  
Physical and mechanical properties for hot-pressed  
cordierite(TiO<sub>2</sub> 15 % wt )/ Al<sub>2</sub>O<sub>3</sub> fibres - composites obtained  
from sonogels.

| Sample  | Dr<br>(%) | no<br>(%) | Hot-pressing |          |          |  | Strength (MPa) |        | Young's modulus<br>(GPa) |       | No. of<br>tests |
|---------|-----------|-----------|--------------|----------|----------|--|----------------|--------|--------------------------|-------|-----------------|
|         |           |           | T(°C)        | P(bar)   | t(min)   |  | Mean           | Range  | Mean                     | Range |                 |
| CT15A60 | 86        | 22        | 910          | 25       | 20       |  | 87.93          | 85-98  | 26                       | 23-28 | 2               |
| CT15A60 | 84        | 24        | 915<br>1200  | 25       | 30<br>60 |  | 81.23          | 75-90  | 23.30                    | 20-28 | 3               |
| CT15A50 | 90        | 16        | 915          | 25       | 25       |  | 74.14          | 56-94  | 24.27                    | 17-30 | 3               |
| CT15A50 | 89        | 17        | 915<br>1200  | 25       | 25<br>60 |  | 61.27          | 53-73  | 20                       | 14-26 | 3               |
| CT15A40 | 93        | 14        | 912          | 25       | 20       |  | 82.30          | 79-85  | 32                       | 31-32 | 2               |
| CT15A40 | 91        | 15        | 912<br>1200  | 25<br>-- | 20<br>60 |  | 77.53          | 71-83  | 26.70                    | 25-28 | 2               |
| CT15A30 | 95        | 9         | 920<br>1200  | 25       | 25<br>60 |  | 74.87          |        | 24.40                    | 20-27 | 3               |
| CT15A20 | 99        | 1.5       | 920          | 25       | 30       |  | 97.15          | 86-108 | 43.30                    | 40-46 | 2               |
| CT15A20 | 98        | 2         | 920<br>1200  | 25<br>-- | 30<br>60 |  | 68.30          | 66-70  | 26.70                    | 25-28 | 2               |
| CT15A10 | 99        | 0.7       | 920<br>1200  | 25<br>-- | 25<br>60 |  | 92.37          | 80-104 | 36.32                    | 33-40 | 2               |

- The residual porosity of samples increases with the volume fraction of fillers .
- The samples with  $\mu$ -cordierite matrix show higher densities than those where  $\alpha$ -cordierite was formed.

This behaviour in  $D_r$  for CT15Zx and CT15Ay composites is in accordance with experimental evaluations of  $D_r$  in the separate cordierite matrix.

#### 4.2.1.3. Samples produced by HIP

The uniaxial compression strength of CT7A35 samples 2.5 x 2.5 x 5 mm of dimensions was tested previously for the hot-pressed CT7A35 composite , and furtherly for the same CT7A35 sample treated by HIP.

The temperature of the hot-pressing was 900 °C and the temperature of the HIP process was 1400°C.

The tests were carried out at high temperature with the axial compression load.

The values of the compression strength obtained are shown in the Table 6 and were higher compared to those obtained from the bending test at room temperature. Thus for hot-pressed CT7A35 at 913°C the strength was 378 MPa and decreased gradually up to 63 MPa when the temperature of the test was increased to 1308°C.



Table 6

Uniaxial compression strength at high temperatures for C7A35  
hot-pressed (hp) and HIPed samples

| Temperature<br>(°C)       | 913 | 949 | 1222 | 1308 |
|---------------------------|-----|-----|------|------|
| $\sigma$ (hp)<br>(MPa)    | 378 | 331 | 182  | 63   |
| $\sigma$ (HIPed)<br>(MPa) | --- | 455 | 218  | 60   |

The highest strength , 455 MPa , was obtained for a CT7Aa composite treated by HIP and the compression test was performed at 949°C

## II.Composites obtained by infiltration of ceramic felts

The nomenclature of these samples will be distinguished from others by denoting by "f" the nature of the reinforcing ceramic felt phase . (e.g. CT15Zf<sub>35</sub> will denote a sample containing 35 % vol zirconia felt with a cordierite (TiO<sub>2</sub> 15 wt %) sonogel matrix).

Dr values obtained for these composites can be seen in Table 7 , they were in perfect agreement with earlier experimental results commented before .

In this case Dr increases with the total volume fraction of the infiltrated matrix , and a slight decrease of Dr was observed when the crystalline  $\alpha$ -form appeared.

### 4.2.2. Thermal Expansion

The average thermal expansion coefficient of cordierite between 25 and 1000 °C is :

$$\alpha = 3.5 \cdot 10^{-6} \quad \text{to} \quad 1.7 \cdot 10^{-6} \quad ^\circ\text{C}^{-1}$$

The expansion coefficients from hot-pressed samples prepared in different conditions were obtained . They are shown in Tables 8a for CT15Zx composites , 8b for CT15Ay , 8c for composites obtained from infiltration of ceramic felts

**Table 7**  
Physical and mechanical properties for cordierite-infiltrated ceramic felts

| Matrix | Cumulative matrix vol fraction (%) infiltrated |      |     |     | Dr (%) | n <sub>o</sub> (%) | Hot-pressing |          |           | Strength (MPa) | Young's Modulus (GPa) |
|--------|--|------|-----|-----|--------|--------------------|--------------|----------|-----------|----------------|-----------------------|
|        | 1st  | 2nd  | 3rd | 4th |        |                    | T(°C)        | P(bar)   | t(min)    |                |                       |
| CT15   | 57   | 81   | 90  | 95  | 99     | 2                  | 915          | 40       | 25        | 96.10          | 41.60                 |
| CT15   | 56   | 70   | 77  | --  | 98     | 6                  | 930          | 40       | 20        | 108.20         | 46.90                 |
|        |  |      |     |     | 97     | 7                  | 930<br>1200  | 40<br>-- | 20<br>60  | 112.00         | 43.17                 |
| CT15   | 57.6   | 80.6 | --  | --  | 97     | 4                  | 910          | 40       | 30        | 119.07         | 55.26                 |
|        |  |      |     |     | 96     | 6                  | 910<br>1250  | 40<br>-- | 30<br>300 | 94.75          | 40.25                 |
| CT15   | 58.6   | --   | --  | --  | 94     | 8                  | 915<br>1250  | 40<br>-- | 20<br>300 | 94.50          | 28.50                 |
|        |  |      |     |     | 99     | 2                  | 920<br>1200  | 40<br>-- | 30<br>60  | 138.75         | 57.13                 |
| CT7    | 64   | 85   | 94  | --  | 99     | 2                  | 915<br>1250  | 40<br>-- | 25<br>300 | 105.00         | 40.00                 |
|        |  |      |     |     | 98     | 2                  | 920<br>1250  | 40<br>-- | 30<br>300 | 63.50          | 29.10                 |
| CT7    | 63   | --   | --  | --  | 97     | 4                  | 920<br>1250  | 40<br>-- | 30<br>300 | 57.70          | 19.60                 |

, and 8d for cordierite samples prepared from melt fusion , hot-pressing from powders and sol-gel techniques.

In Tables 8a and 8b it can be observed that the thermal expansion of composites decreases for higher temperatures and longer heat treatment soaking times.

In general, the thermal expansion coefficient decreases for higher volume fractions of fillers up to 30 vol %. These values were  $3.14 \cdot 10^{-6} \text{ }^{\circ}\text{C}^{-1}$  for CT15Z30 and  $4.55 \cdot 10^{-6} \text{ }^{\circ}\text{C}^{-1}$  for CT15A30 , between 20 and 980°C.

Table 8c shows the evolution of  $\alpha(20-980^{\circ}\text{C})$  for infiltrated and hot-pressed ceramic felt samples heat-treated at temperatures ranging between, 900°C to 1250°C

The matrix of these samples was a CT15 sonogel and the number of infiltrations was 4 , which introduced a volume fraction of matrix higher than 90 % .

The thermal expansion for these samples was similar to that for other composites prepared with short fibres , and ranged between  $8.32$  to  $3.51 \cdot 10^{-6} \text{ }^{\circ}\text{C}^{-1}$  for the following heat-treated conditions : 900°C for 30 minutes and 1250°C for 6 hours , respectively.

Finally , in Table 8d we made a comparison of thermal expansion coefficients for the following samples :

1. Cordierite-glass, (a commercial sample submitted by Corning which was heat treated at 1200°C for 5 hours.
2. Cordierite glass obtained from crushed powders of the

commercial glass , then hot-pressed at 900°C , 25 bar and furtherly heat-treated at 1200°C for 3 hours.

3. CT7 , obtained from sonogels, hot-pressed at 900°C , 25 bar for 15 minutes then heat-treated at 1250°C for 6 hours.

The lowest value obtained for the expansion coefficient for these samples was  $1.20 \cdot 10^{-6} \text{ }^{\circ}\text{C}^{-1}$  , it corresponded to the commercial devitrified glass.

Hot-pressed cordierite showed a coefficient expansion very similar to that from cordierite sonogel containing 7 wt % of titania ,  $3.12 \cdot 10^{-6}$  and  $3.28 \cdot 10^{-6} \text{ }^{\circ}\text{C}^{-1}$  respectively .

All samples were totally devitrified except CT7 at 900°C . The coefficient for this sample was  $4.11 \cdot 10^{-6} \text{ }^{\circ}\text{C}^{-1}$ .

**Table 8**

Thermal expansion coefficient for cordierite( $\text{TiO}_2$  15 % wt)-based composites with : (a)  $\text{Al}_2\text{O}_3$  fibres ;(b)  $\text{ZrO}_2$  fibres ;(c) $\text{ZrO}_2$  ceramic felt and (d) pure cordierite glass (Corning) ; hot-pressing from glass powder ; and cordierite ( $\text{TiO}_2$  7 % wt sonogel)

**Table 8a**

| Sample  | Heat Treatment          |      | $\alpha_{20}^{980}$<br>( $10^6$ ) (a)<br>( $^{\circ}\text{C}^{-1}$ ) |
|---------|-------------------------|------|--|
|         | T( $^{\circ}\text{C}$ ) | t(h) |  |
| CT15A10 | 1250                    | 1    | 5.07   |
| CT15A20 | 1250                    | 1    | 4.56   |
| CT15A30 | 1200                    | 1    | 4.55   |
| CT15A35 | 1200                    | 3    | 4.90   |
| CT15A40 | 1200                    | 1    | 5.73   |
| CT15A50 | 1200                    | 1    | 6.04   |
| CT15A60 | 1200                    | 1    | 7.60   |
|         | 1250                    | 6    | 5.70   |

**Table 8b**

| Sample  | Heat Treatment          |      | $\alpha_{20}^{980}$<br>( $10^6$ ) (a)<br>( $^{\circ}\text{C}^{-1}$ ) |
|---------|-------------------------|------|--|
|         | T( $^{\circ}\text{C}$ ) | t(h) |  |
| CT15Z10 | 1250                    | 6    | 3.96   |
| CT15Z20 | 1250                    | 6    | 3.36   |
| CT15Z30 | 1250                    | 6    | 3.14   |
| CT15Z40 | 1250                    | 6    | 3.54   |
| CT15Z50 | 1250                    | 6    | 4.27   |
| CT15Z60 | 1200                    | 3    | 5.06   |

**Table 8c**

| Sample              | Heat Treatment          |      | $\frac{980}{20}$<br>$(10^6) \text{ (a)}$<br>$(^{\circ}\text{C}^{-1})$ |
|---------------------|-------------------------|------|---|
|                     | T( $^{\circ}\text{C}$ ) | t(h) |   |
| CT15Zf <sub>4</sub> | 1250                    | 6    | 3.51  |
|                     | 1200                    | 1    | 4.01  |
|                     | 900                     | 1/2  | 8.32  |

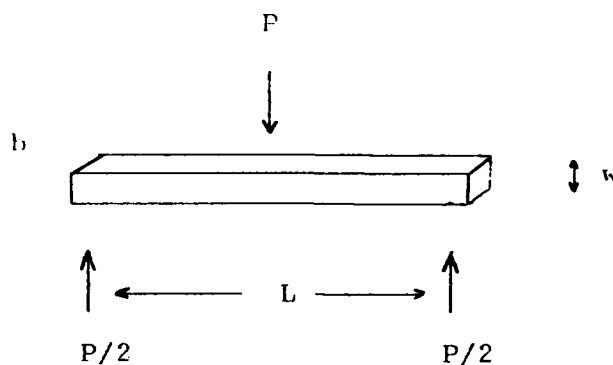
**Table 8d**

| Sample   | Heat Treatment          |      | $\frac{980}{20}$<br>$(10^6) \text{ (a)}$<br>$(^{\circ}\text{C}^{-1})$ |
|--|-------------------------|------|---|
|  | T( $^{\circ}\text{C}$ ) | t(h) |   |
| Bulk glass<br>(Corning)                        | 1200                    | 3    | 1.20  |
| Hot-pressed<br>from powdered<br>glass(Corning) | 1200                    | 3    | 3.12  |
| CT7<br>(Sorogel)                               | 900                     | 1/4  | 4.11  |
|  | 1250                    | 6    | 3.28  |

### 4.3. Mechanical Properties

The flexural strength of composites was determined using an INSTRON 1195 testing machine with a cross-head speed of 0.5 mm/min.

Young's modulus of samples was obtained from the load-deflection curves from the bending test.



Flexural strength and Young's modulus were obtained from the following equations:

$$\sigma = \frac{2 P L}{3 b w^2} \quad E = \frac{P L^3}{4 \delta w^3 b}$$

Where :  $P$  , is the load at failure

$L$  , the distance between cylindric supports

$b$  , the width of the specimen

$w$  , the thickness of the specimen

$\delta$  , the deflection of the sample

The dimensions of the specimens were  $w = (2-3)$  mm ,  $b = 4$  mm and length 15 mm . The distance between supports  $L$  , was



12 mm. The surfaces of samples were previously polished using 6-12  $\mu$ m diamond paste.

In order to have a reference for experimental values in mechanical strength for cordierite , the flexural strength of glass-cordierite specimens prepared from melt was measured . These samples provided by Corning , heat-treated at 950°C or 1150°C for 2-3 hours to develop the  $\mu$ - and  $\alpha$ - crystalline polymorphic forms of cordierite.

The strength and Young's modulus obtained are shown in Table 9.

The corresponding values for Co , CT7, CT11 and CT15 matrices and some CoZx , CoAy and CT7Ay composites samples were presented in Table 3.

Tables 4 and 5 showed the mechanical properties obtained for CT15Zx and CT15Ax composites respectively.

The following observations concerning these results can be made

Table 9.- An increase in mechanical resistance was obtained when crystalline phases were developed in cordierite glass samples.

Table 3.- Samples with titania content higher than 11 wt % showed the lowest strength both for glass and crystalline cordierite matrix. The maximal strength was obtained for a

**Table 9**

Flexural strengths and Young's modulus for cordierite glass (Corning) heat treated at 950 °C and 1150 °C

| Sample         | Strength (MPa) |         |         | Young's Modulus (GPa) |          |       | No. of tests |
|----------------|----------------|---------|---------|-----------------------|----------|-------|--------------|
|                | Mean           | Std.dev | Range   | Mean                  | Std.dev. | Range |              |
| glass          | 80.75          | 5.29    | 73-88   | 26.40                 | 3.98     | 23-35 | 7            |
| $\mu$ -cord    | 134.12         | 22.30   | 98-157  | 32.55                 | 7.72     | 21-43 | 4            |
| $\alpha$ -cord | 137.80         | 22.47   | 106-158 | 35.44                 | --       | 29-35 | 3            |

Instron calibration

|                  |       |      |        |       |     |       |   |
|------------------|-------|------|--------|-------|-----|-------|---|
| SiO <sub>2</sub> | 97.20 | 9.74 | 87-107 | 62.38 | 6.4 | 55-69 | 4 |
|------------------|-------|------|--------|-------|-----|-------|---|

CT11 sample hot-pressed at 950°C with the metastable  $\mu$ -cordierite form.

It can also be observed that mechanical resistance decreases with the degree of conversion of  $\mu$ -cordierite into  $\alpha$ -cordierite.

Tables 4 and 5.- showed that the strength values ranged from 61.27 MPa for a CT15A50 composite up to 107.40 MPa for a CT15Z20 composite ; the Young's modulus varied between 20 GPa for CT15A50 to 43 GPa for CT15A20 composite

A clear and general dependence of mechanical characteristics on volume fractions of fillers was not observed.

Devitrification of the matrix influenced strongly the mechanical strength of composites. In general , we observed a decrease in mechanical resistance (5-10 %) in samples where the matrix was crystalline.

Relative densities and mechanical characteristics obtained for hot-pressed samples prepared from Corning cordierite glass are shown in Table 10 , from which the following observations were made:

- mechanical strength and Young's modulus obtained for glass-cordierite hot-pressed samples were very similar to those obtained by sol-gel techniques.
- The strength values for composites prepared from powders of recrushed commercial cordierite glass and containing a

volume fraction of fibres equal to 20 % , were 10-35 % higher than for identical samples prepared from sonogels.

e.g.:

- cordierite( $ZrO_2$  20 vol %)

Commercial

Strength : 168 MPa at 900°C  
128 MPa at 1150°C

CT15 Sonogel

107.40 MPa at 908°C

- cordierite( $Al_2O_3$  20 vol %)

Commercial

Strength : 110 MPa at 900°C  
76 MPa at 1150°C

CT15 Sonogel

97.15 MPa at 920°C  
68.30 MPa at 1200°C

If we compare these mechanical characteristics with those obtained in previous studies for CT7 and CT11 based composites (in Table 3a) , it can be concluded that the optimal quantity of  $TiO_2$  nucleant was around 10 % wt. for cordierite sonogels. The presence of higher quantities (15 wt %) of titania , was the main cause of the weakness observed in mechanical properties.

All these observations were concurred in good agreement with relative densities obtained and shown in §4.2.2.1.

The fracture surfaces of fractured specimens were observed with a JEOL JSM-6300F S.E.M. microscope; the samples were previously etched in 4 % HF solution for 30-60 s.

**Table 10**

Physical and mechanical properties for hot-pressed cordierite-based composites obtained from mixing the powdered glass (Corning) and ceramic fibers.

| Sample           | Dr<br>(%) | no<br>(%) | Hot-pressing |          |           | Strength<br>(MPa) | Young's<br>Modulus<br>(GPa) |
|------------------|-----------|-----------|--------------|----------|-----------|-------------------|-----------------------------|
|                  |           |           | T(°C)        | P(bar)   | t(min)    |                   |                             |
| cord             | 100       | --        | 906          | 20       | 20        | 89.40             | 27.43                       |
| cord             | 99        | 2.15      | 906<br>1150  | 20<br>-- | 20<br>180 | 57.55             | 22.75                       |
| CZ <sub>20</sub> | 100       | 0.24      | 900          | 20       | 15        | 168               | 59                          |
| CZ <sub>20</sub> | 95        | 8.80      | 900<br>1150  | 20<br>-- | 15<br>180 | 128               | 41                          |
| CA <sub>20</sub> | 100       | 0.14      | 900          | 20       | 15        | 110               | 51                          |
| CA <sub>20</sub> | 96        | 12        | 900<br>1150  | 20<br>-- | 15<br>180 | 76                | 38                          |

From these observations the quality of the matrix-fibres interfaces was evaluated. It was good in certain zones and inexistent in others for the same sample. This also revealed a great porosity caused by some heterogeneous aggregates of fibres in bundles which were the origin of weak points which lead to failure.

The fracture surfaces of infiltrated ceramic felts showed a very homogeneous matrix dispersion , an absence of porosity and better matrix-fibres interface . All these observations were in good agreement with mechanical observations for these samples.

Vickers' microhardness was determined from sintered or hot-pressed cordierite samples and composites . The experimental values obtained are shown in Table 11.

Table 11

Vickers' microhardness for a) hot-pressed cordierite with TiO<sub>2</sub> 11 and 15 wt % content and cordierite from powdered glass (Corning) for hot-pressed at 900 °C and then(\*)heat treated at 1200 °C for 3 hours;(b) hot-pressed mixtures of fibres and powdered glass matrix and (c) CT15-based composites

All the specimens were treated between 900-950°C for 30 minutes except that designated by (\*) which was treated at 1200°C for 3 hours

| 11a                             |                 | 11b              |                 | 11c                  |                 |
|---------------------------------|-----------------|------------------|-----------------|----------------------|-----------------|
| Sample                          | Hv<br>(Vickers) | Sample           | Hv<br>(Vickers) | Sample               | Hv<br>(Vickers) |
| CT11                            | 717 ± 24        | CZ <sub>20</sub> | 816 ± 35        | CT15Z <sub>20</sub>  | 866 ± 82        |
| CT15                            | 937 ± 57        | CA <sub>20</sub> | 790 ± 12        | CT15Z <sub>40</sub>  | 596 ± 11        |
| Corning<br>hot-press.<br>Powder | 758 ± 35        |                  |                 | CT15A <sub>40</sub>  | 877 ± 92        |
| *Corning<br>hot-press<br>Powder | 817 ± 80        |                  |                 | CT15A <sub>40</sub>  | 572 ± 35        |
|                                 |                 |                  |                 | CT15Zf <sub>30</sub> | 961 ± 30        |
|                                 |                 |                  |                 | CT7Zf <sub>40</sub>  | 917 ± 53        |

## 5. SYNTHESIS OF SILICA SONOGEL MATRICES FOR OPTICAL APPLICATIONS



It has been shown [7] that semiconductor doped-glasses are composite materials with interesting optical applications because of their considerable optical nonlinearities and fast relaxation times. Devices based on these materials may be useful in optical switching and for optical logic.

Semiconductor fine particles included in insulating matrices have been recently prepared and studied [8,9]. A collection of tiny Cd(Se,S) crystallites were embedded in glass matrices ensuring a deep confining potential for both electrons and holes in the microcrystallites. These inclusions are possible to be considered as spherical particles with a small dispersion of the radii, thus providing a description of the physical properties in these materials as a function of the crystallite size.

In a semiconductor microcrystallite with a radius over 10 Å, discrete subbands are formed in valence and conduction bands since electron and hole wave functions are confined. The effective gap between the top of the valence subband and the bottom of the conduction band being a function of microcrystallite size. This is called the quantum size effect and the experimental result is that the optical absorption lines shift as a function of the microcrystallite sphere radius.

The viability of the sol-gel process in the preparation of monolithic SiO<sub>2</sub> xerogels at very low temperature , provides high porosity host matrices with a narrow pore size distribution to be used as support for fine semiconductor particles.

In this part of the work pure "sono" and classic silica gels were prepared to be used as the host matrix for CdS small-sized particles formed in gels by precipitation chemical reactions.

For CdS the quantum size effect occurs as the crystallite diameter is comparable or below the Mott-Wannier exciton size (around 50-60 Å).

### 5.1. Physical and Optical Requirements.

The main requirements needed to obtain a stabilized matrix for these extremely fine particles were:

- the presence of a fine texture and porosity  
(pore diameter < 50 Å )
- physical and mechanical stability : the structure of the matrix must withstand the variations of temperature under experimental conditions.(15-25°C)
- optical transmission : the surface of these materials must be polished to provide optical quality.

## 5.2. Study of Chemical and Physical Parameters

Several chemical and physical parameters have a marked influence on the final texture of the gel.

They are the following:

### Chemical Parameters

1. Type of silicon alkoxide precursor (TEOS or TMOS)
2. Molar ratio of hydrolysis water , ( $R_w = \text{mol water/mol Alkoxide}$ )
3. pH
4. Presence of organic solvents
5. Presence of drying control chemical additives (DCCA's)
6. Use of polymeric organic additives.

### Physical Parameters

7. Ultrasonic dose
8. Gelation conditions
9. Aging and drying conditions

1. The gels were prepared starting from two different silicon alkoxide precursors : tetramethoxysilane (TMOS) and tetraethoxysilane (TEOS).

2. It was observed in other works that higher  $R_w$  values close to 10 ensured a complete hydrolysis and consequently a higher porosity. The  $R_w$  used in this study was equal to 3 , 4 , or 10.

3. Different pH were tested in order to obtain a fine final texture of gels.

4. Alcoholic solvents were used only for preparing the classic gels. The alcoholic solvent was chosen according to the alkyl group of the alkoxide. Thus methanol was used with TMOS and ethanol with TEOS. The quantity of the solvent was fixed at 50 vol % / vol alkoxide.

5. The presence of DCCA's controls the drying process, thus avoiding the fracture of the gel network and providing a narrower pore size distribution.

Formamide (FOR) and dimethyl formamide (DMF) were used as DCCA's. The mol ratio of DCCA/mol silicon alkoxide was designated as  $R_{for}$  and  $R_{dmf}$  respectively and varied as follows:

$$R_{for} = 3, 4 \text{ or } 7$$

$$R_{dmf} = 2$$

6. Some organic additives were used in order to test their influence on the texture and mechanical characteristics of gels.

The organic substances employed were: polyethyleneglycol (PEG) tetraethyleneglycol (TEG) and polydimethylsiloxane (PDMS).

7. Two different ultrasonic doses were employed leading to low-dosed (LD) and high-dosed (HD) sonogels. The doses employed were 50 and 250  $Jcm^{-3}$  respectively.

8. The gelation temperatures varied from 20 to 50°C.

9. The aging process was made at different temperatures ranging from 20 to 40°C. The aging time varied from 2 to 168 hours. Drying was carried out at 20-60°C with soaking time varying from 24 to 500 hours.

All the experimental parameters employed are shown in Table 12.

### 5.3.Experimental Procedure

The host gels were prepared by submitting the mixture of silicon alkoxide and water acidified with  $\text{HNO}_3$  to various doses of ultrasonic radiation with a 600W sonifier (SONIC MATERIALS , USA) operating at 20 KHz with a 13 mm diameter titanium transducer driven by an electrostrictive device. Insonation was carried out in a glass beaker 70 mm in diameter kept in a thermostatted bath at 20°C.

Two different alkoxyde precursors were used to obtain the starting sol , tetraethoxysilane (TEOS) and tetramethoxysilane (TMOS).

The hydrolysis reaction was completed under the action of ultrasounds in a time which varied from a few seconds (for TMOS with  $R_w=10$  ) to 4-5 minutes (for TEOS with  $R_w=4$ ). The temperature of the solutions reached 70°C during insonation.

The pH of hydrolysis water varied from zero to 1.5 .

**Table 12**

Starting precursors and different chemical and physical parameters employed in the preparation of the SiO<sub>2</sub> host gels for semiconductor nanoparticles

| PRECURSOR<br>ALKOXIDE | DCCA<br>(mole/mole<br>SiO <sub>2</sub> ) | ORGANIC<br>ADDITIVE<br>(vol/vol Alk)% | RH <sub>2</sub> O<br>(pH) | ULTRASOUND<br>DOSE<br>(J cm <sup>-3</sup> ) | AGING        |           | DRYING       |           | (% mole Cd(NO <sub>3</sub> ) <sub>2</sub><br>per mol SiO <sub>2</sub> ) |
|-----------------------|--|---------------------------------------|---------------------------|---|--------------|-----------|--------------|-----------|---|
|                       |  |                                       |                           |   | t<br>(hours) | T<br>(°C) | t<br>(hours) | T<br>(°C) |   |
| TEOS<br>TMOS*         | FOR<br>(3,4,7)                           | None                                  | 4,10<br>(0, 1.5)          | 250   | 2-168        | 20-40     | 24-500       | 20-60     | 1,5,8,10,15,30,40   |
|                       |  | (15)<br>PEG (20)<br>(30)              |                           |   |              |           |              |           |   |
|                       |  | TEG (30)<br>(50)                      |                           | 50  |              |           |              |           |   |
|                       |  | ETOH(50)<br>MeOH(50)*                 |                           | No  |              |           |              |           |   |
|                       | DMF<br>(2)                               | None<br>PEG (20)                      |                           | 250   |              |           |              |           |   |
|                       |  |                                       |                           |   |              |           |              |           |   |

Sonosolutions with different compositions were then obtained by adding DCCA's in the following proportions:

$$R_{for} = 3, 4 \text{ or } 7 \text{ or } R_{d\#f} = 2. .$$

The final solution was homogenized under ultrasonic action introducing an energy varying from 50 to 250 Jcm<sup>-3</sup> to the whole volume of solution. The pH of the final solution was equal to 2.

In some cases certain organic additives were added , (PEG) , TEG and PDMS in a 20,30 and 50 vol % of the precursor's volume.

Finally x mol of Cd(NO<sub>3</sub>)<sub>2</sub> 4H<sub>2</sub>O /mol SiO<sub>2</sub> , with x = 15 , 30 and 40 were added to the different solutions. Cadmium salt was added under the action of ultrasounds in some cases and with mechanical agitation in others.

Classical SiO<sub>2</sub> gels were prepared by adding 50 vol % of EtOH to TEOS or of MeOH to TMOS solutions , per volume of silicon alkoxide. The hydrolysis reaction and the dilution of cadmium nitrate were obtained by mechanical agitation for a total time of 15 minutes.

The final solutions were poured into hermetic plastic containers of 19 mm edge or hermetic cylindric plastic containers of 20 mm diameter.

The gelation was induced in a range of temperatures varying from 20 to 40°C . The times of gelation varied from 2-

3 hours , for samples prepared using TMOS with  $R_w=10$  and  $R_{for}=3$  , sonified with  $250 \text{ Jcm}^{-3}$  and  $T_{gel}=40^\circ\text{C}$  , to several weeks for samples where DMF was employed as DCCA.

One week later after gelation , the containers were open and the samples left to dry in the ambient atmosphere. The drying of the gels continued for 1 month.

The optimal  $\text{SiO}_2$  sonogel matrices were prepared following the diagram shown in Fig. 3 which indicates the compositions of the starting materials selectioned.

The samples prepared by this method were denoted as TMx or TEx depending on the type of alkoxide used in their preparation , (TM for TMOS and TE for TEOS) , x being the molar percent of  $\text{Cd}^{2+}$  added in respect to  $\text{SiO}_2$  .

After drying the transparent xerogels were put in contact with  $\text{H}_2\text{S}$  vapour produced by decomposition of thioacetamide (TAA). Two different methods were employed for the diffusion of  $\text{H}_2\text{S}$  into the porous structure of the gels :

In the first method the gels were placed in hermetic containers containing TAA at  $35-40^\circ\text{C}$ . Exposure times varied from 24 hours to 1 week . The resulting gels obtained were coloured ranging from light transparent yellow to opaque orange , as the result of the  $\text{CdS}$  particles precipitated inside the pores of the gels.



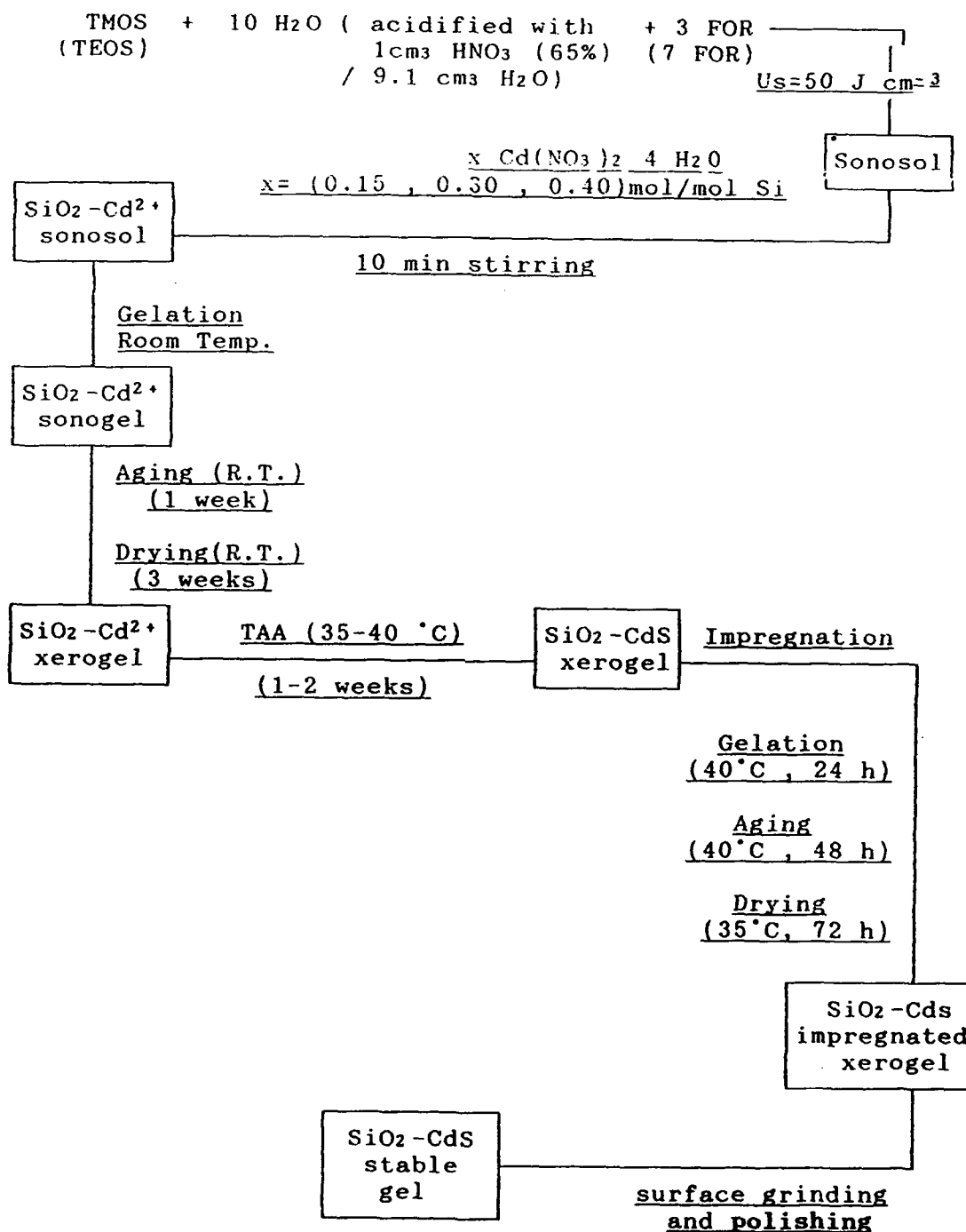


Figure 3

Schematic route for preparing SiO<sub>2</sub>-CdS sonogels

In the second method TAA was placed in a glass container and decomposed at 80-100°C , the resulting H<sub>2</sub>S vapour was passed along a circulatory system driven by an air current , as shown in Fig. 4 , and maintained under 0.5 Kg cm<sup>-2</sup> in contact with the gel samples.

After diffusion the samples were stabilized by two different procedures:

- Thermal stabilization
- Impregnation

#### 5.4 Thermal Stabilization

The SiO<sub>2</sub>-CdS doped gels were treated at 40 , 70 and 80°C for 24 hours and then stocked in a dry atmosphere at 20°C.

#### 5.5. Impregnation Procedure

The need for clear and transparent surfaces for optical applications makes it essential to polish the samples.

This process is difficult because the high residual porosity presented in the surface of the xerogels and the weakness of the silica network formed. The combination of both factors results in a poor transmission of visible light after polishing.

The impregnation process [10] results in the pores in the surface of the gel being sealed , which improves mechanical

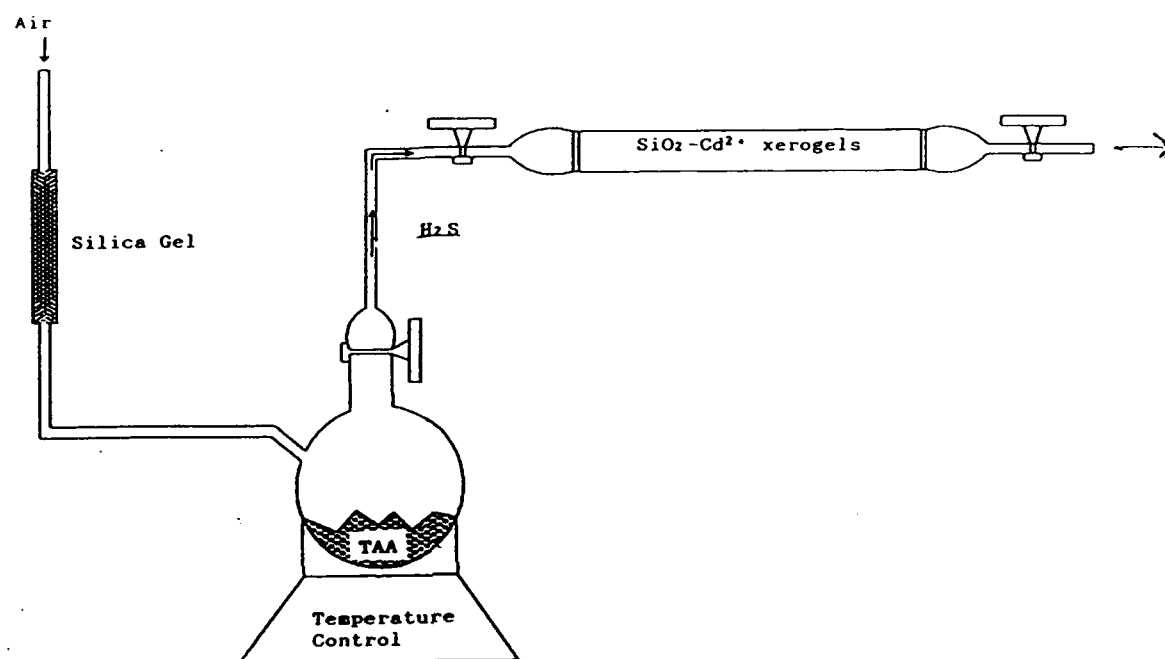


Figure 4. Diffusion treatment system for  $\text{SiO}_2\text{-Cd}^{2+}$  xerogels

and physical stability of the samples and thus provides optical transparence after polishing .

The impregnation of  $\text{SiO}_2\text{-CdS}$  samples was carried out by total immersion of the gel sample in a sonosol of the same composition as the host gel.

The optimal impregnation procedure was the following :

a) The samples were placed in the impregnating sonosol which contains 25 mole %  $\text{Cd}^{2+}$  respect to  $\text{SiO}_2$  .The temperature of the sonosol was around 20 - 25°C.

b) The samples were left submerged in the solution under reduced pressure (Pr) with the following schedule (Table 13):

Table 13

| Time(min) | Pressure(mm Hg) |
|-----------|-----------------|
| 0         | 760             |
| 1         | 80              |
| 3         | 60              |
| 5         | 40              |
| 7         | 20              |
| 15        | 20              |
| 17        | 760             |

The samples remained in the vacuum jar for 30 minutes before being returned to room temperature

c) The impregnated sample was then removed and the rest of the solution which remained at the surface of the sample was dried with a filter paper. The specimen was then introduced

into a hermetically closed container and put in the oven at 40°C for 48 hours to promote gelation of the sealing solution. After this time the cover was removed and the impregnated gel was left to dry at 35°C for 72 hours.

The sample was then ready for polishing. This was carried out first with a grinding paper (P600 or P1000) to obtain parallel surfaces then with a silk cloth and diamond paste (1  $\mu\text{m}$  grain size). The resulting samples presented a good transmission of visible light (90 % transmitted light)

#### *5.5.1. Experimental Observations on the Impregnation Process*

The CdS doped SiO<sub>2</sub> xerogels were partially transparent due to the presence of some impurities on the surface of the samples after exposure to H<sub>2</sub>S. The polishing treatment was necessary to render the specimens totally transparent for optical experimentation.

In the case of non-impregnated samples the surface was insufficiently polished, scattering phenomena were observed with subsequent loss of optical transparency quality. The impregnation of these samples gave satisfactory results after polishing, leading to transparent samples for optical studies.

The conservation of these samples required a well established environmental conditions as follows:

1. Humidity : 30-40 %
2. Temperature : 18-25°C

If humidity exceeded 50 % , the samples turned opaque because of the water absorbed (impregnation does not seal the total porosity of the gels).

The transparency of the samples can be restored by placing the specimens in a dessicator the time necessary for removing absorbed water.

On the other hand , if the samples are overdried they also lose their transparency (dissolved excess of  $\text{Cd}^{2+}$  salt reprecipitates on the surface of the sample). In order to restore transparency the samples must be placed in a humid environment.

Some important aspects have to be taken into account in order to avoid the crack failure of the samples during the impregnation process:

- 1.-The nature of the impregnating solution
- 2.-The value of the final reduced pressure
- 3.-The gelation process of the sealing solution
- 4.-The drying process of the impregnated sample

1.- A certain minimal quantity of cadmium nitrate must necessarily be present in the impregnating solution in order

to avoid the failure of the samples. We used impregnating solutions containing 25 mol %  $\text{Cd}^{2+}$  in respect to  $\text{SiO}_2$  .

2.- When the final pressure was lower than 20 mm Hg some of the gels failed during impregnation and others failed during the drying process of the impregnated gel.

3-. The samples must be rapidly enclosed in hermetic containers for gelation in order to avoid an excessive and rapid evaporation of solvent which could induce cracking .

4.- Drying must be carried out very carefully after gelation. The temperature must not exceed  $40^\circ\text{C}$  during drying. The time of drying must be 72 hours , as a minimum , before polishing.

## 6. CHARACTERIZATION OF $\text{SiO}_2$ -CdS DOPED GELS



### 6.1. Evolution of Physical Properties

Apparent densities ,( $D_a$ ), linear contraction, ( $l/l_0$ ), and weight losses ( $w/w_0$ ) , were measured before and after the impregnation of CdS doped SiO<sub>2</sub> gels.

The evolution of the apparent density ,  $D_a$  , of these gels during the impregnation process , was measured by Archimedes' method in toluene. Tables 14 and 15 show the evolution of  $D_a$  , porosity , linear contraction and weight losses of different samples , obtained from TMOS , during the impregnation process.

Tables 16a and 16b show the apparent densities for non-impregnated and impregnated CdS-doped gels respectively .The diffusion of H<sub>2</sub>S in these gels was produced by the methods schematized in Fig. 3 and 4.

These values were obtained from geometric calculation of the volume of the samples after polishing.

Higher densities for impregnated samples than for non-impregnated specimens were observed from these measurements.

A higher density was also observed for samples with higher CdS content. Fig.5.

Table 14

Apparent density,  $D_a$ , of TMX samples before impregnation

| Sample | $D_a$<br>( $\text{gcm}^{-3}$ ) | $\Delta l/l_0$<br>(%) |
|--------|--------------------------------|-----------------------|
| TM15   | 1.51                           | 31                    |
| TM30   | 1.57                           | 32                    |
| TM40   | 1.64                           | 32                    |

Table 15

Evolution of physical characteristics for TMX impregnated gels. ( $D_a'$ : apparent density for impregnated gels;  $(\Delta l/l_0)'$  linear contraction and  $(\Delta w/w_0)'$  loss weight of impregnated gels respect to non-impregnated xerogel.

| Sample | Drying |                         | $D_a'$<br>( $\text{gcm}^{-3}$ ) | $(\Delta l/l_0)'$<br>(%) | $(\Delta w/w_0)'$<br>(%) | Aging Time<br>before<br>Impregnation<br>(months) |
|--------|--------|-------------------------|---------------------------------|--------------------------|--------------------------|--|
|        | t(h)   | T( $^{\circ}\text{C}$ ) |                                 |                          |                          |  |
| TM30   | 96     | 30                      | 1.57                            | 1                        | 14                       | 1  |
|        | +24    | 45                      | 1.62                            | 2                        | 20                       |  |
|        | +24    | 60                      | 1.74                            | 8                        | 31                       |  |
|        | +24    | 70                      | 1.80                            | 11                       | 34                       |  |
|        | +24    | 80                      | 1.83                            | 13                       | 39                       |  |
| TM30   | 96     | 30                      | 1.63                            | 4                        | 13                       | 2  |
|        | +24    | 45                      | 1.69                            | 8                        | 18                       |  |
|        | +24    | 60                      | 1.74                            | 12                       | 27                       |  |
|        | +24    | 70                      | 1.82                            | 15                       | 32                       |  |
|        | +24    | 80                      | Cracked                         | --                       | --                       |  |
| TM40   | 120    | 30                      | 1.71                            | 2                        | 13                       | 1  |
|        | +24    | 45                      | 1.74                            | 5                        | 17                       |  |
|        | +24    | 60                      | 1.80                            | 8                        | 25                       |  |
|        | +24    | 70                      | 1.83                            | 10                       | 32                       |  |
|        | +24    | 80                      | Cracked                         | --                       | --                       |  |

Table 16. Apparent ,  $D_a$  , and skeletal ,  $D_s$  , densities for (a) non-impregnated and (b) impregnated CdS-doped SiO<sub>2</sub> xerogels obtained from TEOS or TMOS by sonocatalytic approach.  $V_p$  is the pore volume of the specimens and  $[Cd^{2+}]$  is the molar concentration of cadmium nitrate in the starting solution. (The diffusion of H<sub>2</sub>S in these gels was carried out by the method indicated in Fig.4)

Table 16 a

| Sample | $[Cd^{2+}]$<br>(M) | $D_s$<br>$g\ cm^{-3}$ | $D_a$<br>$g\ cm^{-3}$ | $V_p$<br>$cm^3\ g^{-1}$ |
|--------|--------------------|-----------------------|-----------------------|-------------------------|
| TM1    | $9.5\ 10^{-3}$     | 2.21                  | 1.29                  | 0.323                   |
| TM5    | $4.9\ 10^{-2}$     | 2.25                  | 1.31                  | 0.319                   |
| TM8    | $8.2\ 10^{-2}$     | 2.28                  | 1.33                  | 0.313                   |
| TM10   | $1.0\ 10^{-1}$     | 2.30                  | 1.34                  | 0.311                   |
| TE1    | $6.3\ 10^{-3}$     | 2.21                  | 1.14                  | 0.420                   |
| TE5    | $3.3\ 10^{-2}$     | 2.25                  | 1.13                  | 0.440                   |
| TE8    | $5.4\ 10^{-2}$     | 2.28                  | ---                   | ---                     |
| TE10   | $6.9\ 10^{-2}$     | 2.30                  | 1.20                  | 0.399                   |

Table 16b

| Sample | $[Cd^{2+}]$<br>(M) | $D_s$<br>$g\ cm^{-3}$ | $D_a$<br>$g\ cm^{-3}$ | $V_p$<br>$cm^3\ g^{-1}$ |
|--------|--------------------|-----------------------|-----------------------|-------------------------|
| TM1    | $9.5\ 10^{-3}$     | 2.21                  | 1.42                  | 0.251                   |
| TM5    | $4.9\ 10^{-2}$     | 2.25                  | 1.50                  | 0.222                   |
| TM8    | $8.2\ 10^{-2}$     | 2.28                  | 1.52                  | 0.219                   |
| TM10   | $1.0\ 10^{-1}$     | 2.30                  | 1.54                  | 0.215                   |
| TE1    | $6.3\ 10^{-3}$     | 2.21                  | 1.20                  | 0.381                   |
| TE5    | $3.3\ 10^{-2}$     | 2.25                  | 1.22                  | 0.375                   |
| TE8    | $5.4\ 10^{-2}$     | 2.28                  | 1.24                  | 0.367                   |
| TE10   | $6.9\ 10^{-2}$     | 2.30                  | 1.25                  | 0.365                   |

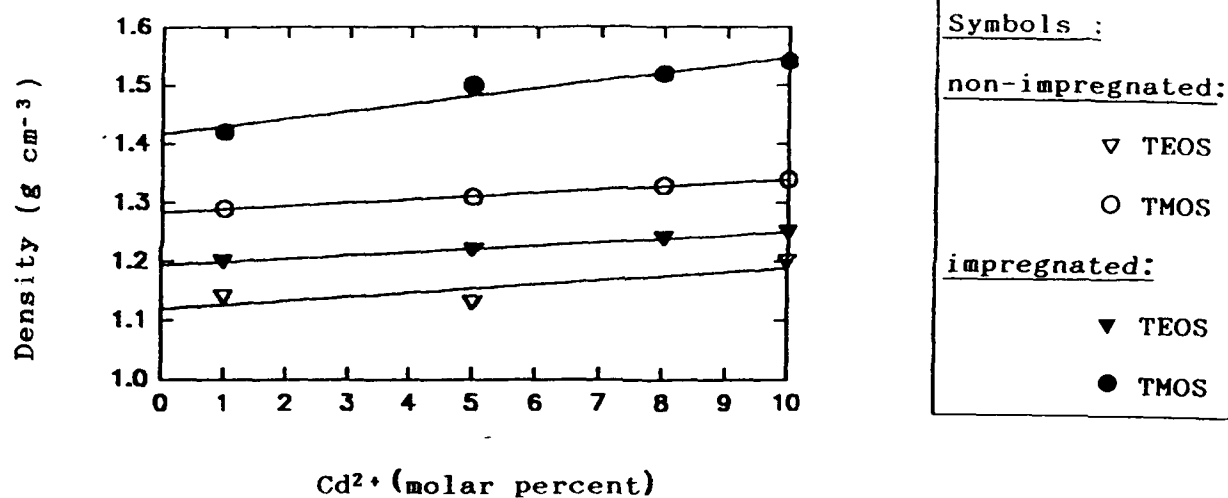


Figure 5. Apparent densities,  $D_a$ , v.s.  $Cd^{2+}$  (molar content) for non-impregnated and impregnated  $SiO_2$ - $CdS$  sonogels.

The pore volume ,  $V_p$  , was obtained from apparent density  $D_a$  and skeletal density  $D_s$  , as follows :

$$V_p = \frac{1}{D_a} - \frac{1}{D_s}$$

The skeletal density was calculated from theoretical densities of the solid phases ,  $D_{SiO_2}$  (2.20 g cm<sup>-3</sup>) , and  $D_{CdS}$  (3.90 g cm<sup>-3</sup>) as follows:

$$D_s = \frac{D_{CdS} D_{SiO_2}}{(1-x) D_{CdS} + x D_{SiO_2}}$$

$x$  being the molar fraction of CdS in the sample

From these values it was also observed that porosity decreased with higher  $Cd^{2+}$  content. Fig. 6 shows this influence of  $Cd(NO_3)_2$  content in the porosity of the gels.

The linear contraction  $l/l_0$  ( Tables 14 and 15) of the samples was measured before the impregnation process and was around 30 %. After the impregnation process an additional linear contraction was found ranging between 1 to 13 % .

An important weight loss , between 13 to 40 % , for TMX samples was observed after the impregnation process.

Other kinds of gels were obtained according to the procedure shown in Fig. 3 but some organic additives such as 20 , 30 or 50 vol % TEG or 15 , 20 or 30 vol % PEG / vol. of the alkoxide , were also added after the hydrolysis reaction.

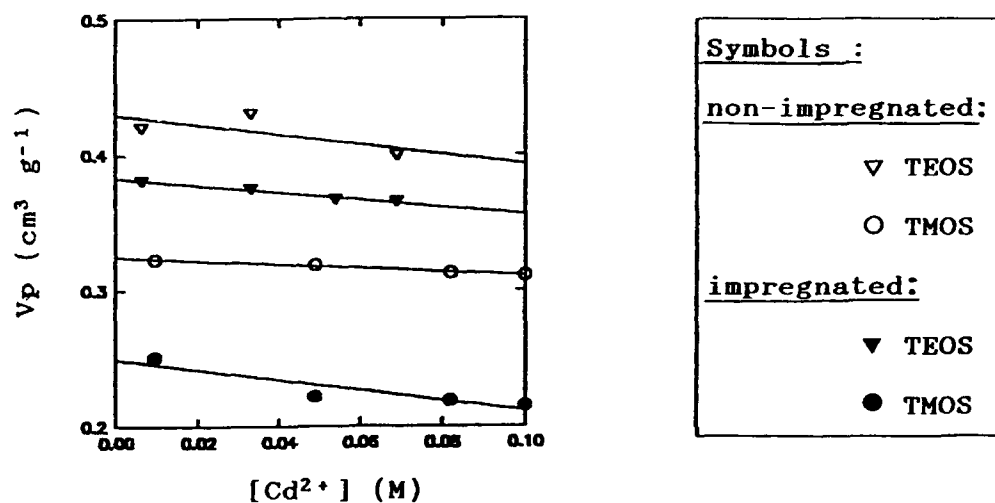


Figure 6. Pore volume ,  $V_p$  , v.s.  $[\text{Cd}^{2+}]$  molar concentration in the starting  $\text{SiO}_2$  sonosol, for non-impregnated and impregnated samples.

The impregnation process of this kind of gel was performed in the conditions indicated in Fig.3.

The composition of the impregnating sonosol was the same as for other gels. Neither TEG nor PEG were added.

This kind of gel presented fracture failure 1 or 2 weeks after polishing.

Classic gels were prepared in the same conditions as those presented in Fig.3 , but adding 50 % vol in MeOH respect to TMOS. Hydrolysis was completed by stirring action and the impregnating sonosol employed was the same as that already described.

We observed that variation in any chemical or physical parameter during gel synthesis drastically influenced the final stability of the gel.

## 6.2. Structural Analysis

### 6.2.1. Thermal Evolution Study

Thermogravimetric (TGA) and differential thermal analysis (DTA) accomplished in nitrogen atmosphere at 10 °C/min , combined with X-ray diffraction analysis , were applied to samples with different  $\text{Cd}^{2+}$  content in order to evaluate physical or structural changes up to 900°C.

TGA from TM15 , TM30 and TM40 samples were carried out in  $N_2$  atmosphere (Fig 7) and we assigned the weight losses as follows:

- 50 -220    evaporation of adsorbed water and organic solvents.
- 250-300    oxidation of organic residues
- 380-450    condensation of residual -OH groups

DTA curves from these samples showed :

- Two endothermic peaks at temperatures lower than 250 °C which were associated with the desorption process.
- An exothermic peak from calcination of organic residues
- An endothermic shoulder from -OH polycondensation
- Exothermic crystallization of  $SiO_2$  at 1300 °C

No exothermic peak , which could indicate the crystallization of CdS , was detected below 900°C. This was probably due to the small concentration of CdS.

Fig. 8 shows the TGA and differential curves (DTG) , as well as DTA for (a) a TE1 composite material stabilized at 80°C and (b) for the pure matrix silica.



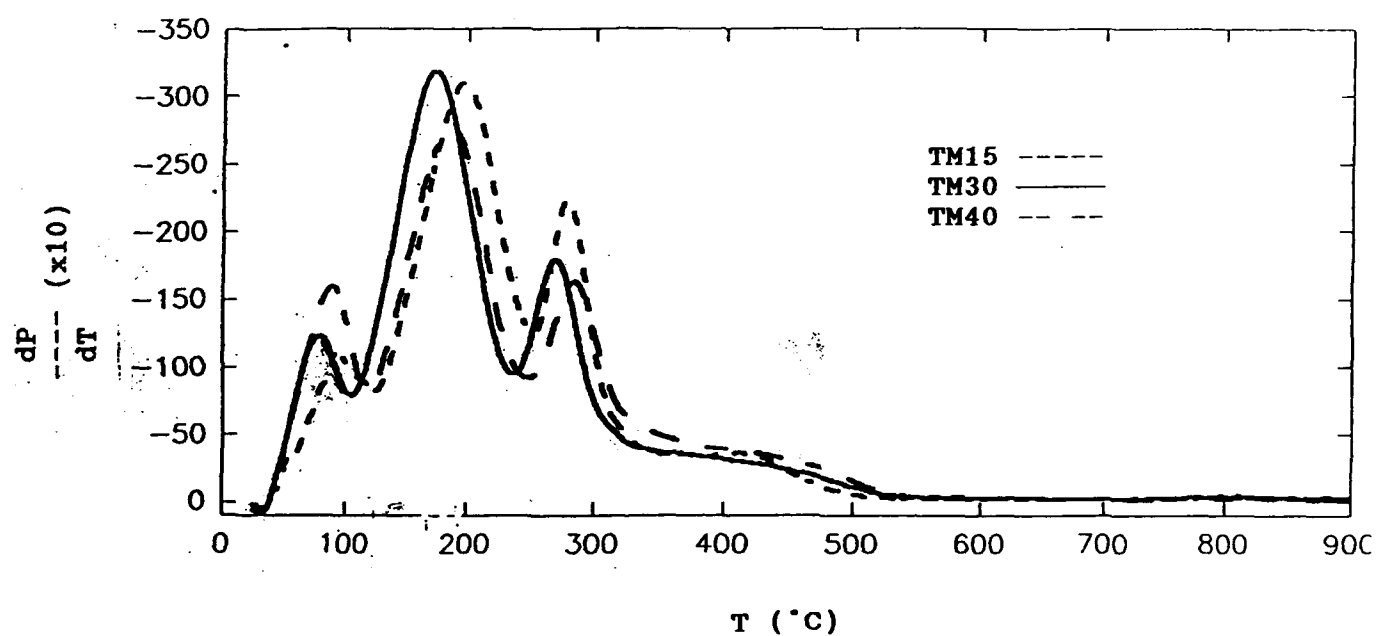
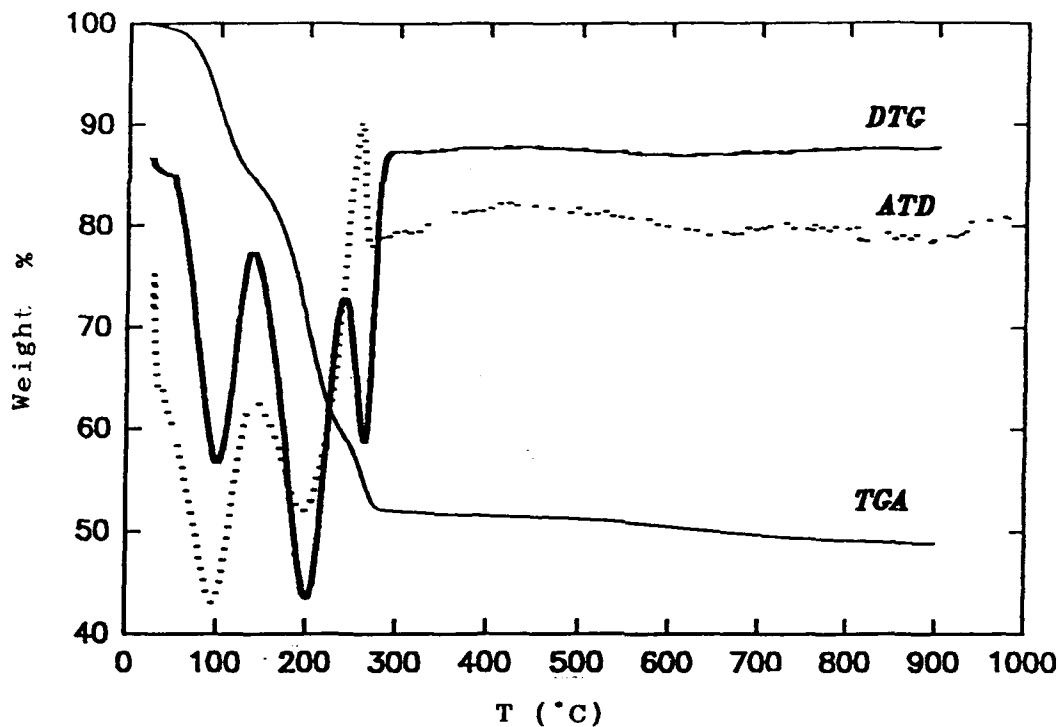


Figure 7. TGA differential curves obtained for TM15 (---) , TM30 (—) and TM40 (- - -) impregnated CdS-SiO<sub>2</sub> sonogels.



8b

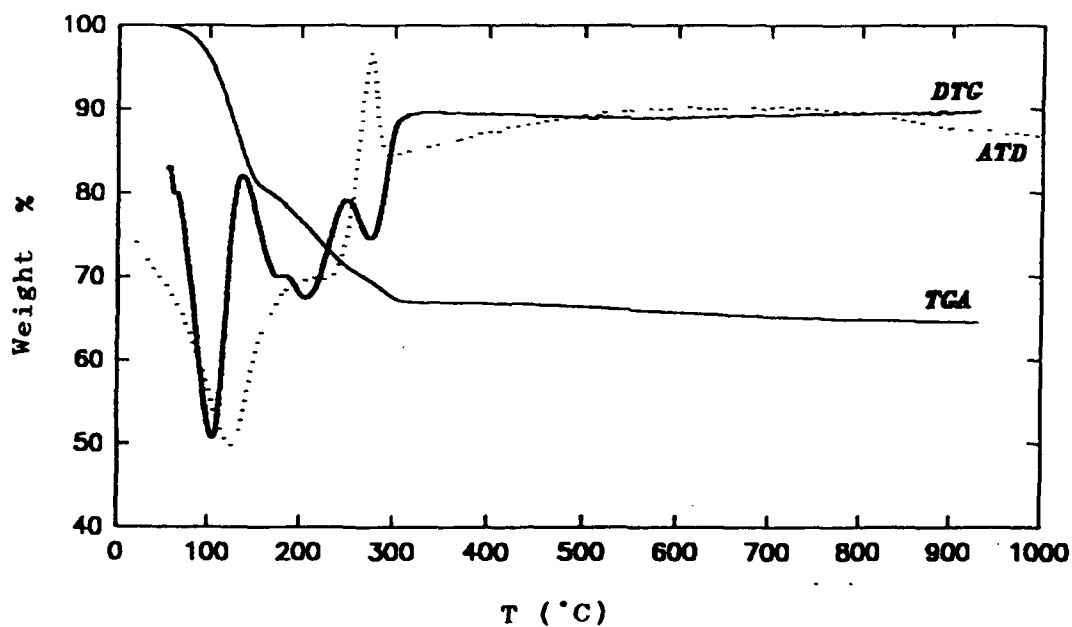


Figure 8. TGA , DTG and DTA curves for (a) TE1 non-impregnated gel stabilized at 80°C and for (b) pure silica xerogel obtained from TEOS , non-impregnated and stabilized at 100°C.

Fig 9 shows the derivative thermograms recorded for TM10 samples at different stages of the preparation process:

(a) non-impregnated pure  $\text{SiO}_2$  sonogel matrix ; (b) non-impregnated CdS-doped  $\text{SiO}_2$  sonogel and (c) impregnated CdS-doped  $\text{SiO}_2$  sonogel. The most remarkable feature observed is that the first weight loss due to desorption of water , ethanol and solvents , decrease after the impregnation treatment. This means that the impregnation reduces the active surface for atmospheric water hydration and therefore the stability of the samples increases.

#### 6.2.2. Textural Features

The evaluation of the nitrogen adsorption measurements by using B.E.T. techniques indicates that the porous structure of these gels was quite uniform , with pore sizes between 10 and 40 Å. This is the standard pore size range usually found for acid catalyzed sonogels (Fig 10).

Some specimens show from the desorption branch a narrower pore size distribution than from the adsorption one. This fact could be explained in terms of the presence of channels linking the pore with the outer structure , which can give rise to "pore blocking" effects. During desorption , pore blocking occurs because bubbles of vapour cannot nucleate at the pressure which would produce capillary evaporation if the pores were freely exposed. Everett [11] has indicates that in a system where pore blocking can occur , pore size distribution curves derived from the desorption branch of the

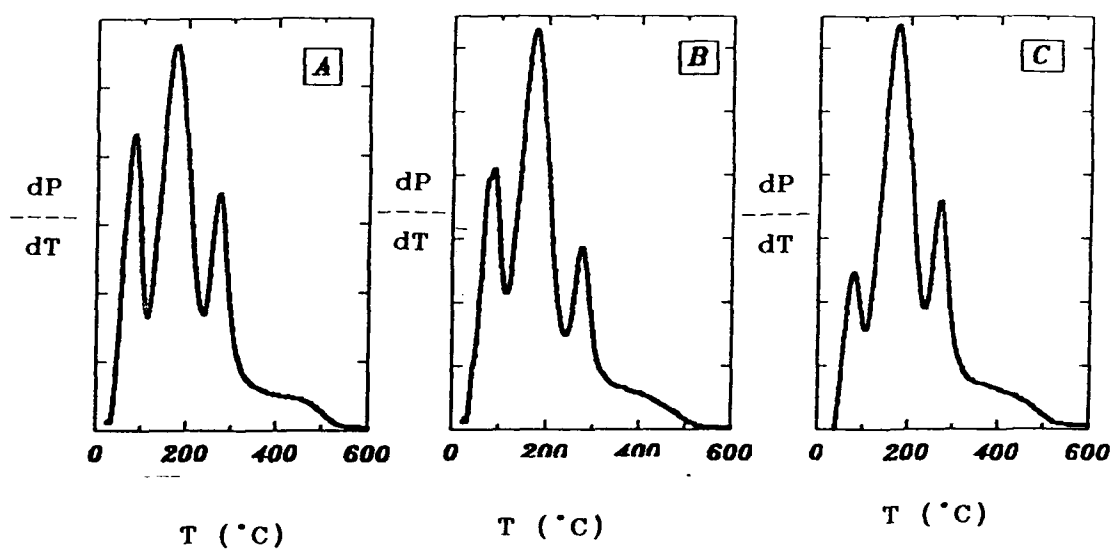


Figure 9. DTG curves for TM10 composite materials: (a) non-impregnated pure silica matrix ; (b) non-impregnated CdS-doped SiO<sub>2</sub> sonogel and (c) CdS-SiO<sub>2</sub> impregnated sonogel.

isotherm are likely to give a misleading picture of the pore structure ; in particular the size distribution will appear to be much narrower than it actually is. The shape of the hysteresis loop corroborates the existence of "ink-bottle" pores.

Fig. 11 shows the N<sub>2</sub>-isotherms and pore size distribution for a non-impregnated TE5 specimen. The sample was previously stabilized at 80°C for 24 hours in an oven , then the specific surface was measured at room temperature at 100°C. The specific surface for TE5 at room temperature was 282 m<sup>2</sup>g<sup>-1</sup> , and the pore volume was 0.22 cm<sup>-3</sup> g<sup>-1</sup>. The same sample at 100°C presented a higher pore volume equal to 0.72 cm<sup>-3</sup> g<sup>-1</sup> , This increase in V<sub>p</sub> at 100°C was due to the evacuation of pores smaller than those evacuated at room temperature.

Fig 11b shows the pore size distribution obtained for this sample at room temperature and at 100°C. No important differences between size pore distributions were observed for TE5 at both temperatures. The porous structure of this material seemed quite uniform with an average pore radius between 10 and 30 Å.

The following results of evaluated specific surface were observed in TM40 impregnated samples:

Specific surface values were 183 m<sup>2</sup>/g for TM40 treated and degased at 120 °C and 14 m<sup>2</sup>/g for the same specimen at room temperature .

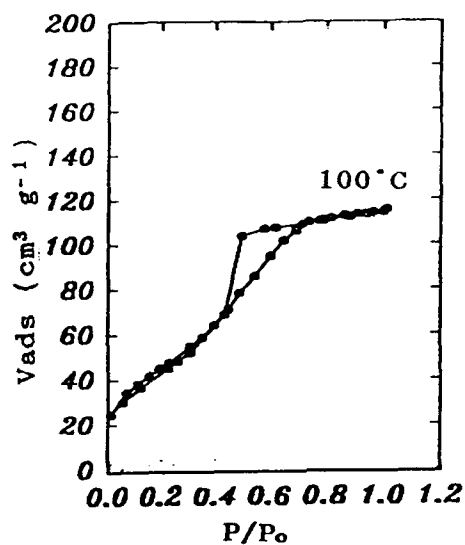


Figure 10a

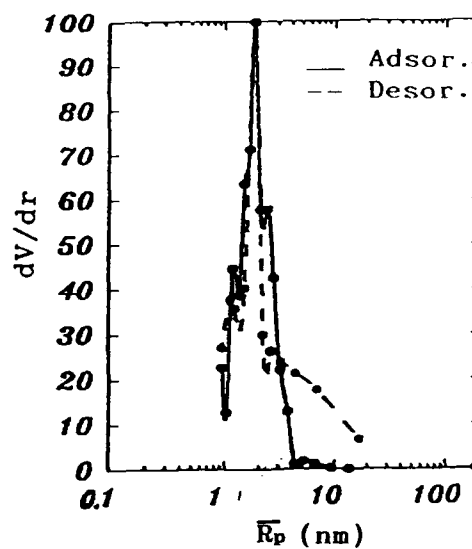


Figure 10b

Figure 10. (a) N<sub>2</sub>-isotherms and (b) pore size distribution, corresponding to a TM10 non-impregnated composite material at 100°C.

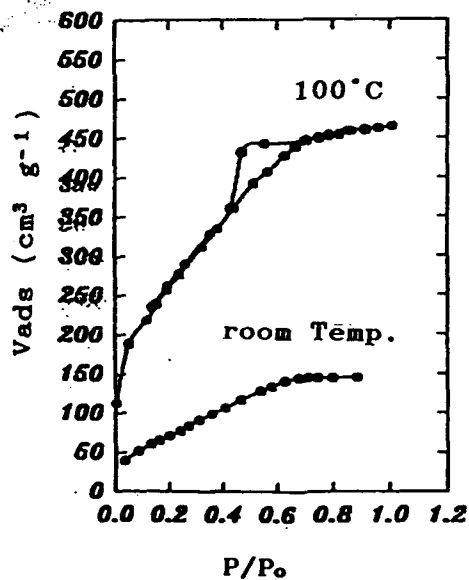


Figure 11a

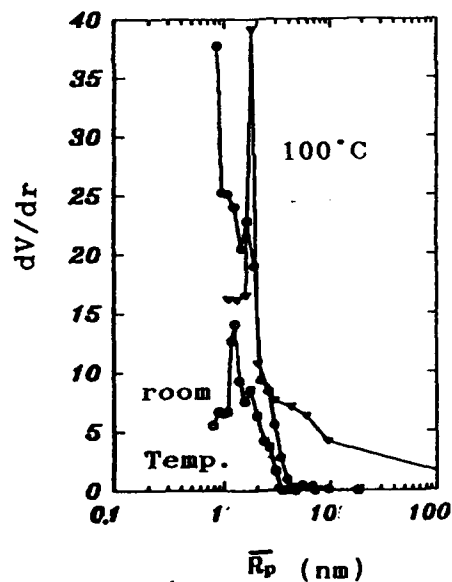


Figure 11b

Figure 11. (a) N<sub>2</sub>-isotherms and (b) pore size distribution at 100 °C and at room temperature in a TE5 non-impregnated composite material previously stabilized at 80°C for 24 hours

At 120°C the TM40 sample showed no particular change in its porous size distribution from TM40 at room temperature.

From these observations it was concluded that the important increase in specific surface was due to the evaporation of interstitial liquids which remained inside the pores of the gel, and that surface increase cannot be associated with a textural modification of the sample.

#### 6.2.3. Transmission Electronic Microscopy

The state of aggregation and average size of CdS particles formed were determined by high resolution transmission electron microscopy (HRTEM) using JEOL JEM-2000 EX microscope, with a structural resolution of 2.1 Å operating at 200 Kv. and with a JEOL JEM-1200 EX operating at 120 Kv. Diffraction electron patterns of these particles were also studied.

Our observations from the JEM-1200 microscope can be summarized as follows:

- An extremely fine and homogeneous background structure of SiO<sub>2</sub>-linked particles (10-20 Å) was present for these samples.

- The sonogels containing organic additives such as TEG or PEG and other samples prepared by classic sol-gel methods presented particles with an average size greater than 15

nm

For these samples CdS hexagonal crystals 50 nm diameter

were also observed

- A very fine and homogeneous dispersion of CdS particles was detected in TEx and TMx samples both with  $R_w=10$  and  $R_{for}=3$

The average size diameter was around 5-10 nm. However CdS hexagonal crystals 30 nm diameter were observed in TM40 samples.

- The CdS particle size distribution with an average diameter of 5 nm was determined from TEM micrographs in TM5 and TM1 specimens. This can be observed in Fig.12.
- Diffraction patterns from microanalysis revealed the presence in a TM5<sub>for</sub> sample of CdS microcrystals in the hexagonal (greenockite) form (ASTM 6-314).

Fig 13 shows TEM micrographs of SiO<sub>2</sub>-CdS composite materials.

The HRTEM observation permitted the visualization of crystalline structure for the semiconductor Cds particles .  
Fig 14.



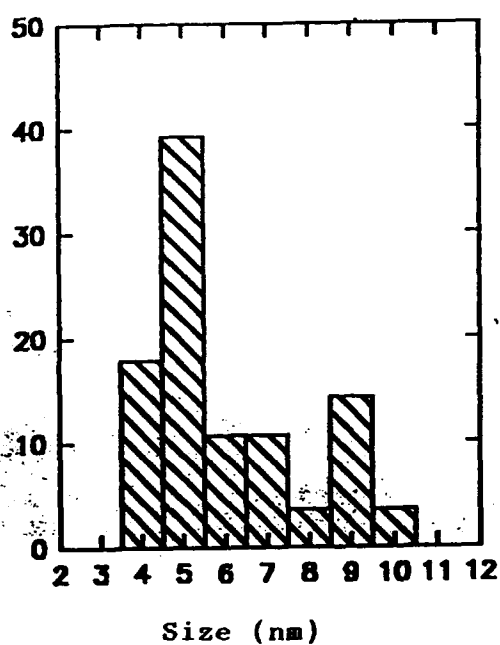


Figure 12a

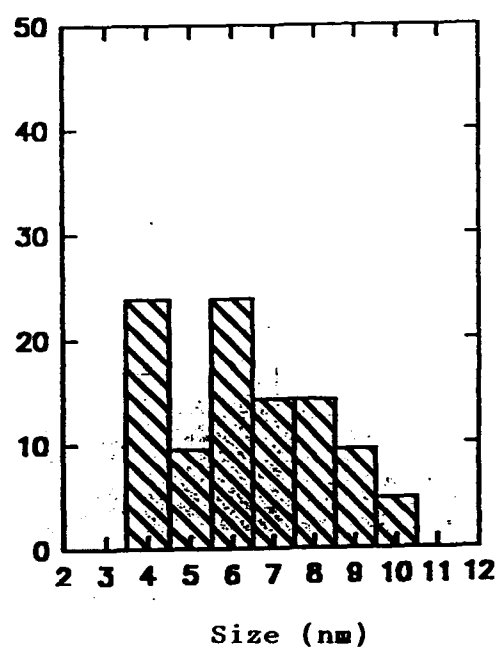


Figure 12b

Figure 12. CdS particle size distributions obtained from HRTEM micrographs for (a) TM5 and (b) TM1, CdS-SiO<sub>2</sub> composite materials.



Figure 13a



Figure 13b

Figure 13. TEM micrographs from (a) TM15 and (b) TM40 CdS-SiO<sub>2</sub> composite materials.

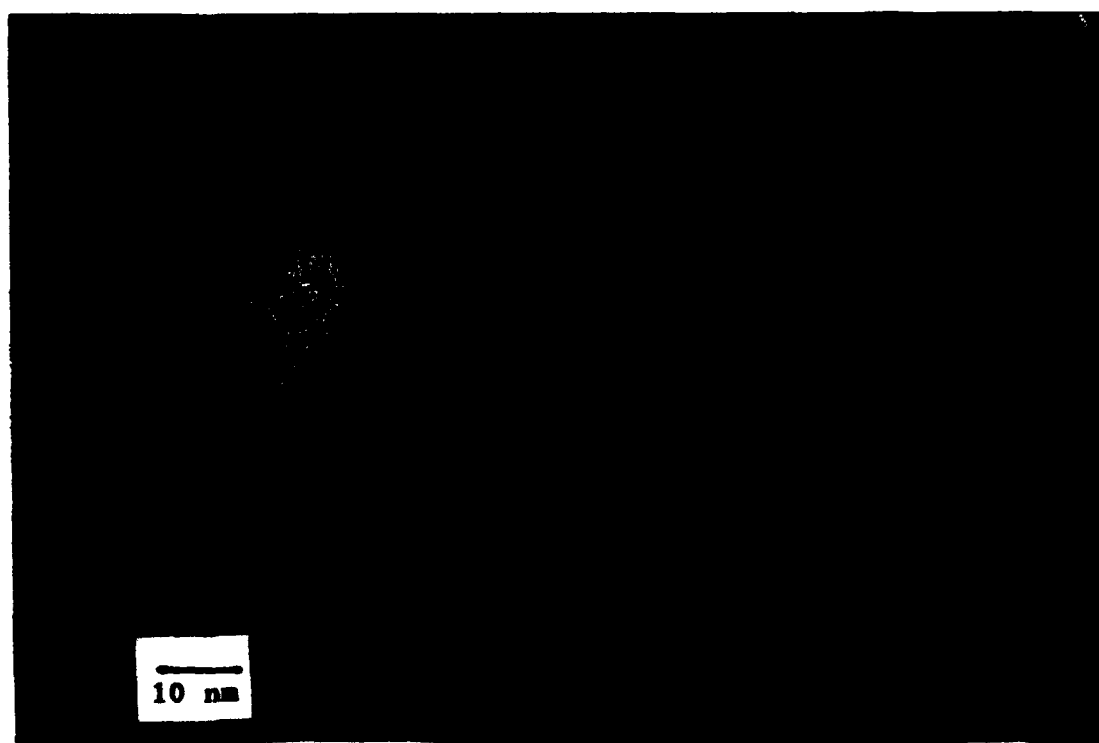
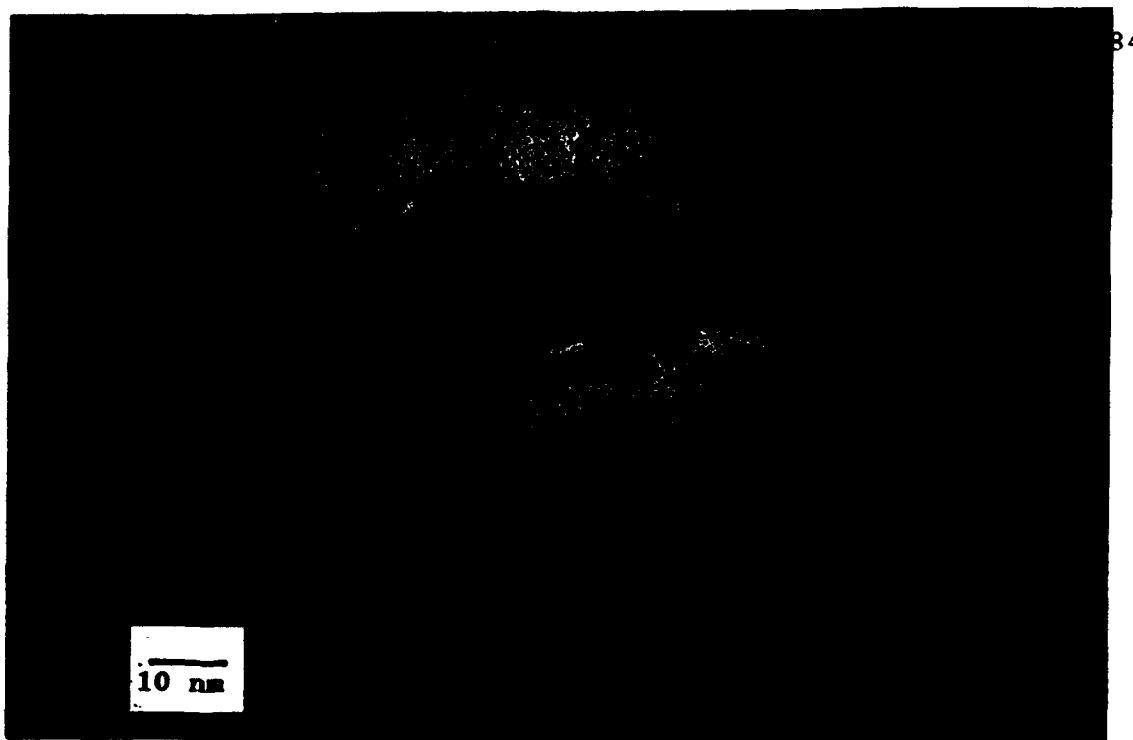


Figure 14. HRTEM micrographs from a TE1 CdS-SiO<sub>2</sub> composite.

#### 6.2.4. SAXS Measurements

Results from TEM observations were combined with small angle X-ray scattering (SAXS) measurements, made using synchrotron radiation in LURE (Orsay) facility. Data were collected in a wide range of the scattering vector modulus  $q(0.01-0.4 \text{ \AA}^{-1})$  around the primary beam.

Three different series of gels were studied by this technique :

They were prepared with a molar ratio TEOS/H<sub>2</sub>O/FOR equal to 1:4:4 and contained 15 mol % of Cd<sup>2+</sup> with respect to SiO<sub>2</sub>.

Different ultrasonic doses were employed : 50 Jcm<sup>-3</sup> (low-dosed (LD)) for the first series, and 250 Jcm<sup>-3</sup> (high-dosed (HD)) for the second series of sonogels.

The third series of gels was obtained by adding 50 volume % ethanol with respect to TEOS to the LD sonogels. These last samples were designated as "classic gels" due to the presence of alcoholic solvent.

The samples were exposed to TAA at 40°C during 6 or 48 hours, thus obtaining gels with low and high exposure times respectively.

The curves of intensity vs. scattering vector modulus,  $q$ , (Fig 15) for these samples show a linear decay characteristic of a low aggregation degree corresponding to a swollen

branched network. The Table 17 shows the slope values of the log-log representation for these specimens. It is remarkable that the slope increases with the concentration of CdS particles in the matrix. This fact is the consequence of the fresh state of the gels at the moment of SAXS measurements. The increase in intensity at small  $q$  is produced by a larger porosity due to the presence of  $\text{Cd}^{2+}$  ions in the  $\text{SiO}_2$  matrix. This behaviour is also detectable on the classic gels. The electrostatic charge effects of  $\text{Cd}^{2+}$  ions inhibit the aggregation process, building a more open structure at  $\sim 300$  Å length scale.

On the other hand sonogel samples show a shoulder near  $0.07 \text{ Å}^{-1}$  which indicates a correlation range of about 45 Å associated with a more homogeneous distribution than those in classic gels. In order to obtain more information, Zimm analysis ( $1/I(q)$  v.s.  $q^2$ ), of the SAXS intensities was made (Fig.16). The gyration radii obtained for sonogels were in agreement with the correlation length due to the shoulder in log-log curves as shown in Table 17. In all cases for high  $q$  values the Zimm representation, presents a deviation from linearity characteristic of spherically shaped arrangements of the clusters grown in the matrix.

#### 6.2.4.1. Titchmarsh Transform

From SAXS data on polydisperse systems, a volume-weighted particle size distribution can be calculated on the assumption of spherically shaped particles from Zimm analysis, by means

of a Titchmarsh transform [12] of the experimental intensity  $I(q)$ . This inversion formula can be applied in a first-order approach if the size of particles is quite different from that of the porous matrix. Another kind of error arises from the fact that the intensities are available only for a finite interval,  $q_{\min} \leq q \leq q_{\max}$ , rather than for all  $q$ . Therefore for high  $q$  values, the intensity corresponds to the effects of electronic density fluctuations due to the internal structure and should not be used.

Experimental data were corrected from spurious background contribution in the curve  $I(q) q^n$  v.s.  $q$ , where  $n$  is the Porod slope in a log-log plot, since it allows a constant limit of  $I(q)q^n$  to be calculated when  $q \rightarrow \infty$ , in order to minimize the cut-off errors in the inversion formula.

Fig.17 show the Titchmarsh transform for sono and classic gels mentioned before. They show a good resolution in sonogels. As it can be observed, the growth of a shoulder is noticeable at about 5 nm, due to the CdS particles in the matrix, which can be considered as the crystallite size. The classic samples seem to have a similar size-distribution for both, CdS crystallites and SiO<sub>2</sub> gel matrix which cannot be distinguished by this method.

Figures 15 , 16 and 17 concern  $\text{SiO}_2\text{-Cd}^{2+}$  (without  $\text{S}^{2-}$  dopant) and  $\text{SiO}_2\text{-CdS}$  gels obtained by three different methods:

- 1.- Low-Dosed gels (LD) , submitted to  $50 \text{ Jcm}^{-3}$  of ultrasonic dose.
- 2.- High-Dosed gels (HD) , submitted to  $250 \text{ Jcm}^{-3}$  of ultrasonic dose.
- 3.- "Classic Gels" , obtained from LD gels by adding 50 vol % EtOH with respect to  $\text{SiO}_2$ .

These gels were classified in three series depending on the method used in power their preparation. Each series consisted of the following three specimens :

- 1.-  $\text{SiO}_2\text{-Cd}^{2+}$  gel without  $\text{S}^{2-}$  dopant
- 2.-  $\text{SiO}_2\text{-CdS}$  gel with low-exposure time (6 h) to TAA vapours at  $40^\circ\text{C}$
- 3.-  $\text{SiO}_2\text{-CdS}$  gel with high-exposure time (48 h) to TAA vapours at  $40^\circ\text{C}$ .

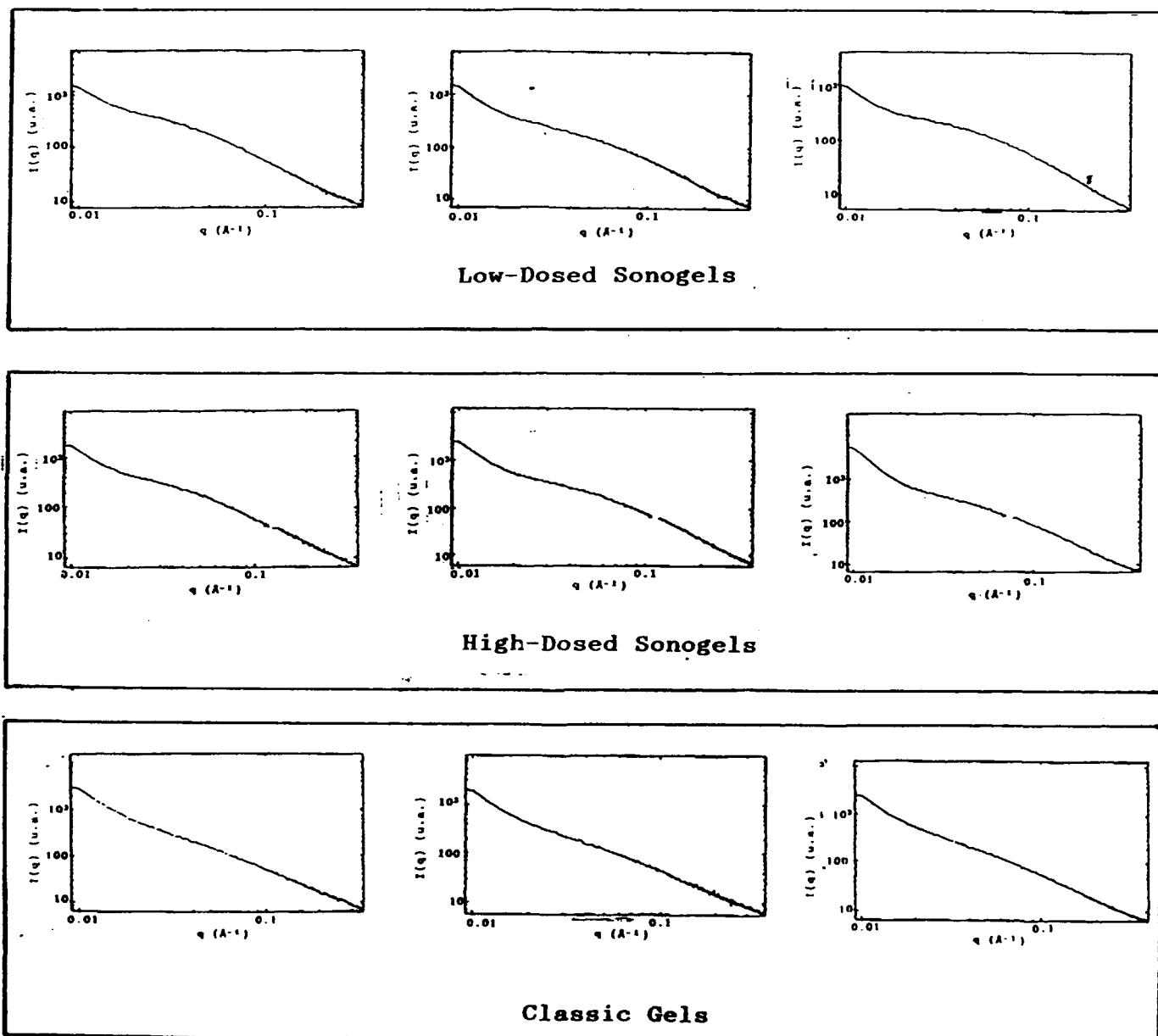
Without  $S^{2-}$  dopantLow exposure  
time to  $H_2S$ High exposure  
time to  $H_2S$ 

Figure 15. Evolution of the diffused intensity,  $I$ , as a function of the scattering vector modulus,  $q$ , for different  $SiO_2-Cd^{2+}$  and  $SiO_2-CdS$  gels.



AD-A238 184

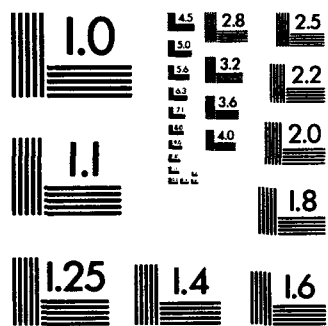
SONOGELS IN THE PREPARATION OF ADVANCED GLASS AND  
CERAMIC MATERIALS(U) MONTPELLIER-2 UNIV (FRANCE)  
J ZARZYCKI 20 OCT 92 AFOSR-TR-92-0981 AFOSR-89-0533

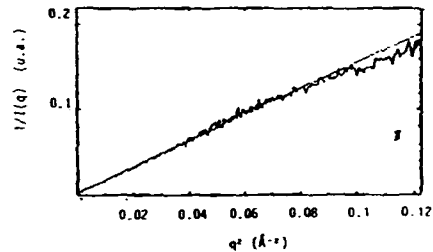
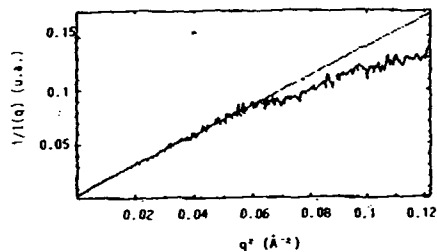
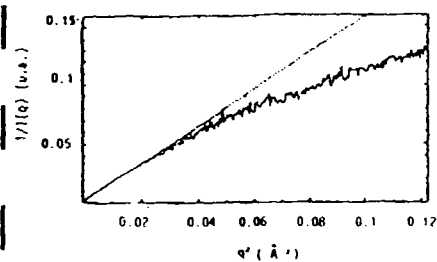
2/2

UNCLASSIFIED

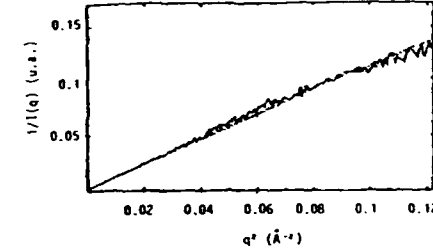
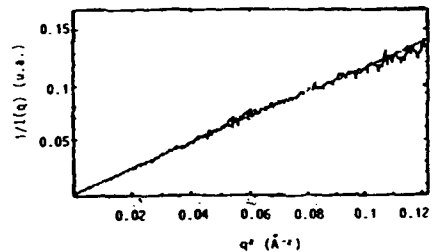
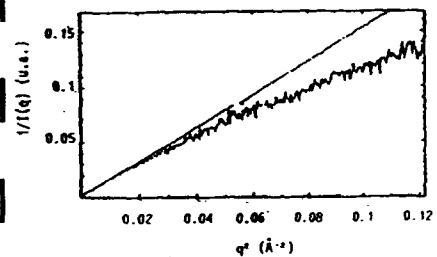
ML

END  
FILMED  
1-92  
DTIC

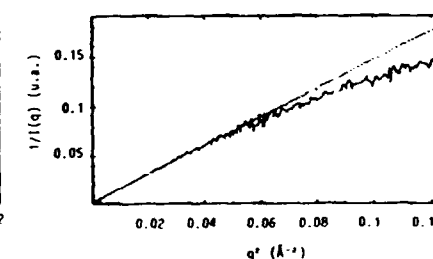
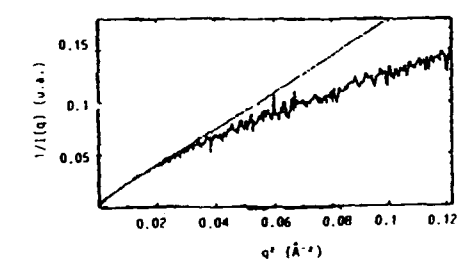
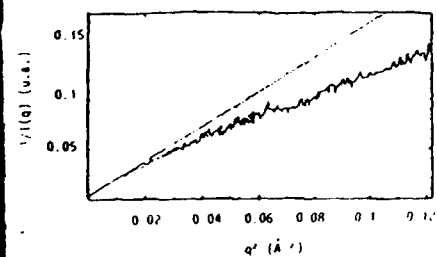


Without S<sup>2-</sup> dopantLow exposure  
time to H<sub>2</sub>SHigh exposure  
time to H<sub>2</sub>S

Low-Dosed Sonogels



High-Dosed Sonogels



Classic Gels

Figure 16. Zimm representation  $1/I(q)$  v.s.  $q^2$ ;

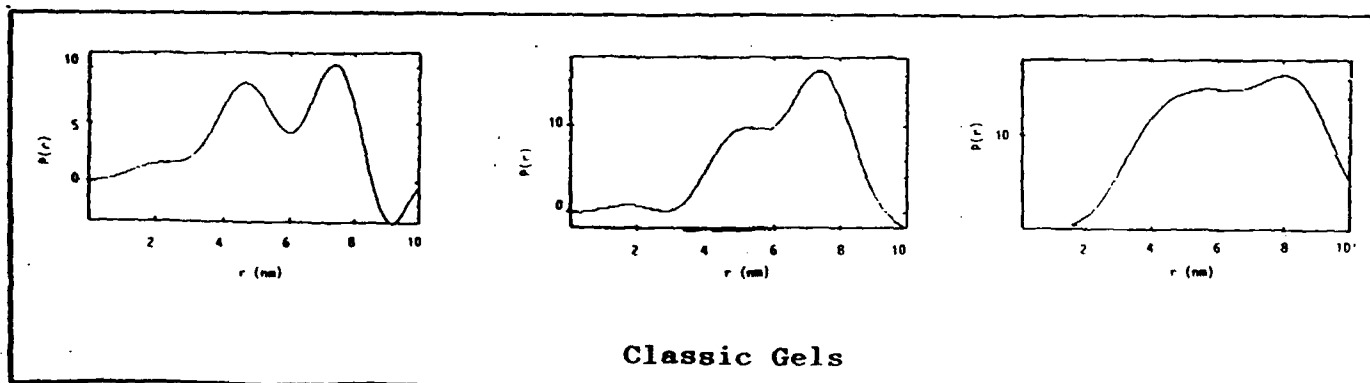
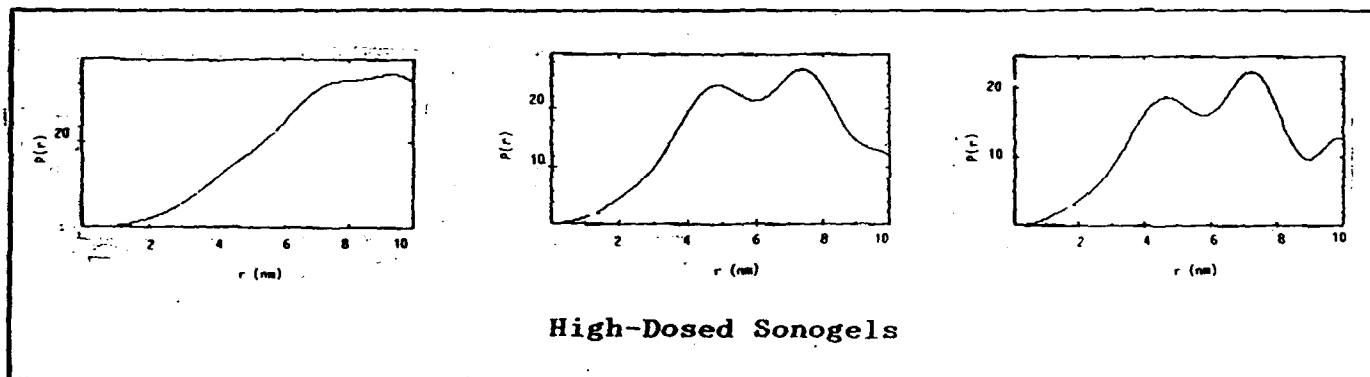
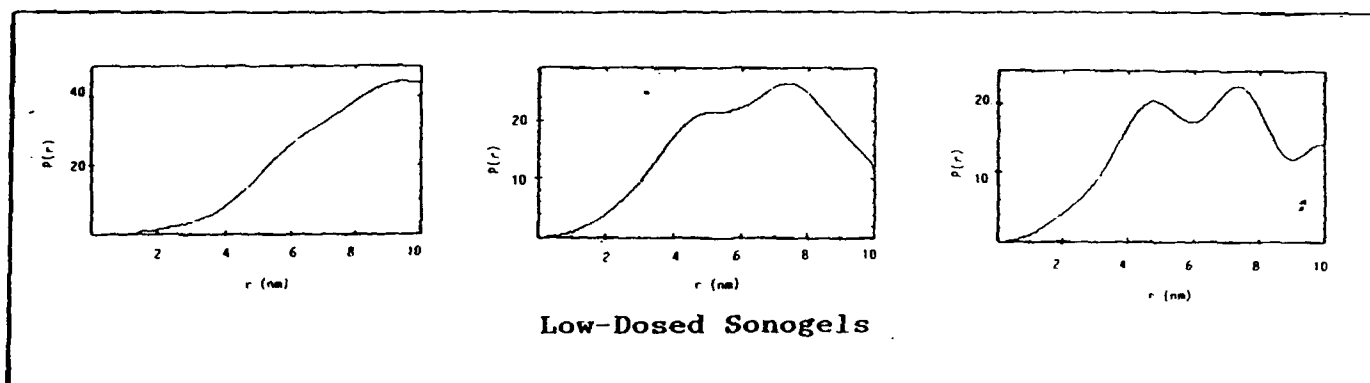
Without  $S^{2-}$  dopantLow exposure  
time to  $H_2S$ High exposure  
time to  $H_2S$ 

Figure 17. Particle-size-distribution ,  $P(r)$  , as a function of the particle radii ,  $r$ ;

Table 17

Correlation length calculated from log-log curves and gyration radii for "sono" and classic SiO<sub>2</sub>-CdS gels.

| Sample              |                                      | log-log<br>slope | Rg (nm)<br>Zimm |
|---------------------|--------------------------------------|------------------|-----------------|
| <u>Classic gels</u> | without<br>dopant                    | 1.60             | 4.4             |
|                     | Low exposure<br>to H <sub>2</sub> S  | 1.52             | 3.5             |
|                     | High exposure<br>to H <sub>2</sub> S | 1.71             | 3.5             |
| <u>LD sonogels</u>  | without<br>dopant                    | 1.63             | 4.5             |
|                     | Low exposure<br>to H <sub>2</sub> S  | 1.80             | 3.4             |
|                     | High exposure<br>to H <sub>2</sub> S | 1.90             | 4.0             |
| <u>HD sonogels</u>  | without<br>dopant                    | 1.69             | 4.8             |
|                     | Low exposure<br>to H <sub>2</sub> S  | 1.92             | 4.4             |
|                     | High exposure<br>to H <sub>2</sub> S | 1.97             | 4.6             |

### 6.3. Optical Characterization

#### 6.3.1. Raman Spectroscopy

The following samples were studied by Raman spectroscopy:

SiO<sub>2</sub>-CdS gels prepared from

- TEOS with  $R_w=4$  ,  $R_{for}=4$  and  $Cd^{2+}(\text{mol } \%)=15$  , designated as TE15<sub>for</sub>
- TEOS with  $R_w=4$  ,  $R_{mf}=2$  and  $Cd^{2+}(\%)=15$  , designated as TE15<sub>mf</sub>
- TEOS with  $R_w=4$  and  $Cd^{2+}(\%)=15$  designated as TE15.

The pH of hydrolysis water was 1.5 and the ultrasonic dose applied was equal to 250 J cm<sup>-3</sup> for all the samples.

From these analysis we observed:

- Weak bands at about 485 and 605 cm<sup>-1</sup> from TE15<sub>for</sub> sample  
These bands suggest the formation of the so-called D<sub>1</sub> and D<sub>2</sub> defects in structure originating from vibrations of cyclic tetra- and trisiloxanes , respectively.
- Spectra from samples TE15<sub>mf</sub> and TE15 only showed the 485 cm<sup>-1</sup> band
- TE15<sub>for</sub> sample presented a line around 610 cm<sup>-1</sup> which denoted the existence of bulk CdS. This peak was not observed in TE15 sample and was strongly displaced

towards  $561\text{ cm}^{-1}$  , probably because of different structure characteristics of each sample.

Raman spectra from TM15 and TM30 impregnated samples showed the same characteristic defect structure bands as in the TE15for sample. The corresponding band for CdS at  $610\text{ cm}^{-1}$  was also observed.

### 6.3.2. Absorption Spectra

The optical absorption spectra of  $\text{SiO}_2\text{-CdS}$  sono and classic samples were measured with a CARY 2300 Spectrophotometer UV-VIS-NIR and with a UV-VIS-NIR , Perkin-Elmer LAMBDA-19 , in the 300-600 nm range

Fig 18 shows the absorption spectra for CdS-SiO<sub>2</sub> doped gels obtained from TEOS or TMOS. The blue shift of the absorption band is clearly visible and we can obtain the exciton energy from the absorption edge. The position of the band evidences that the semiconductor particles sizes fluctuate in the range of the CdS quantum confinement.

In general it was observed that the absorption increases for higher  $\text{Cd}^{2+}$  content. This was expected due to metallic ion concentration increase in the matrix , which becomes more absorbent. Samples with 10 %  $\text{Cd}^{2+}$  show a broader blue shift. Fig. 19 and 20 represent this behaviour in terms of the absorption coefficient.

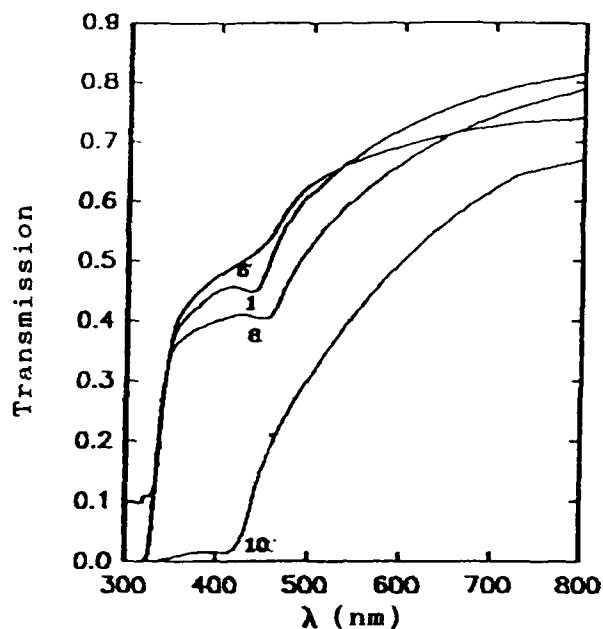


Figure 18a

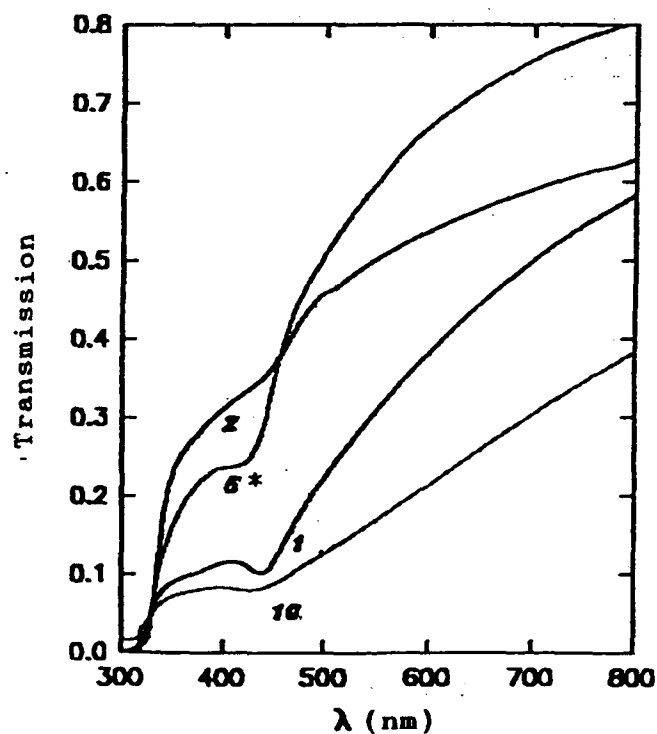


Figure 18b

Figure 18 Absorption spectra for  $\text{SiO}_2\text{-CdS}$  composite materials prepared from : (a) TMOS , (TMX) and (b) TEOS (TEX) .The  $\text{Cd}^{2+}$  mol % , X , is indicated for each spectrum. All the samples were impregnated except the TE5 sample , designated by (\*) , which was stabilized in an oven at  $80^\circ\text{C}$  for 24 hours.



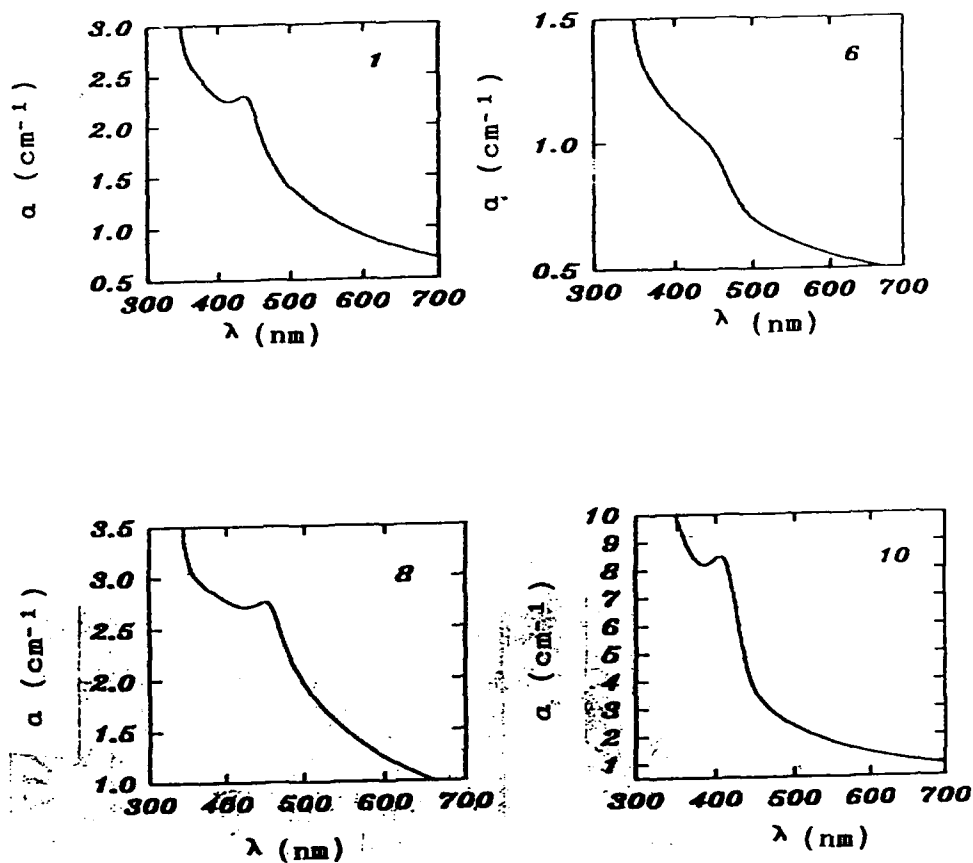


Figure 19. Optical absorption coefficient,  $\alpha$ , v.s. wavelength for  $\text{SiO}_2$ -CdS composite materials prepared from TMOS and with different  $\text{Cd}^{2+}$  mol % contents indicated in the Figure. The absorption spectra correspond to those of Fig 16a.

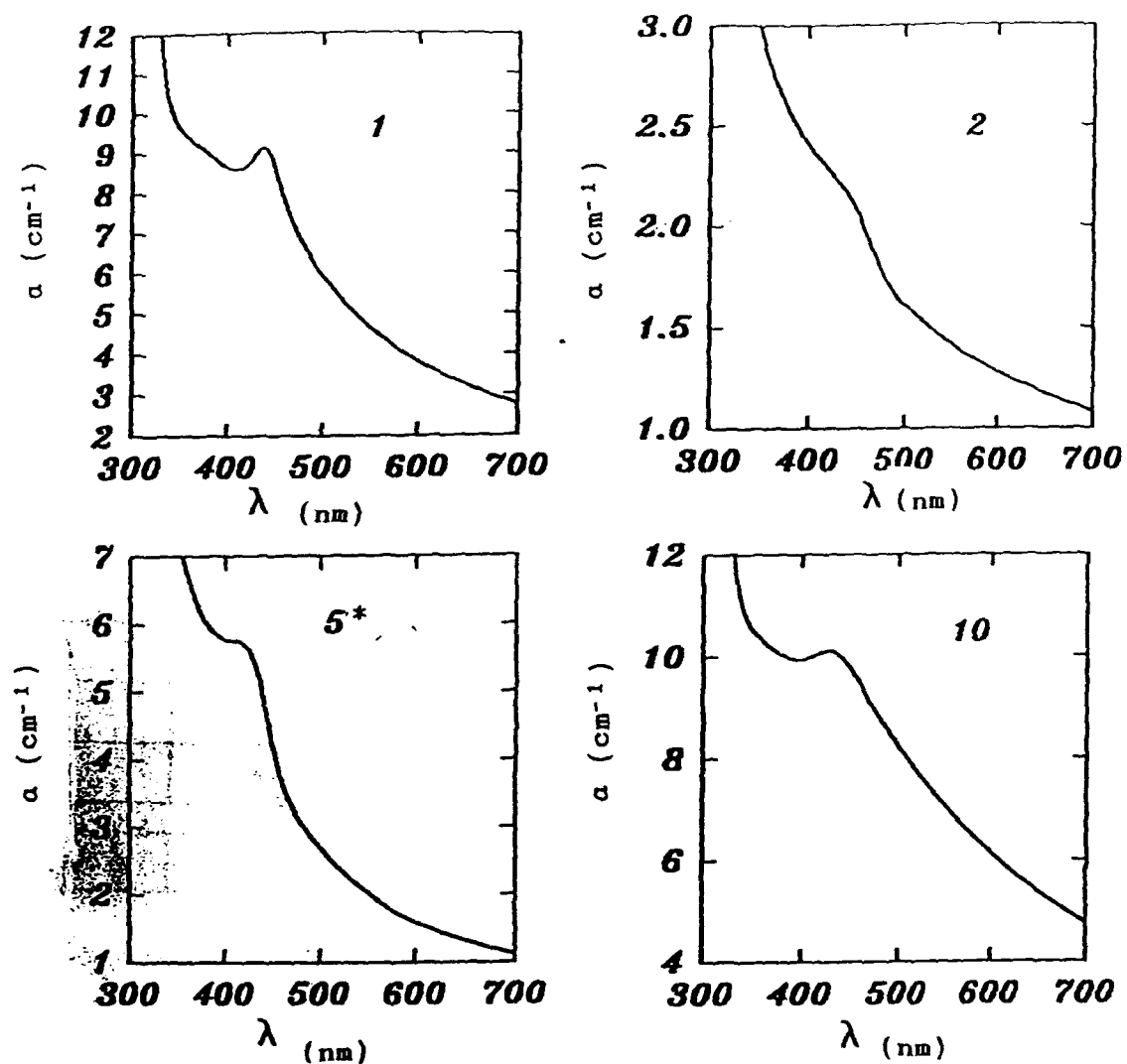


Figure 20.. Optical absorption coefficient ,  $\alpha$  , v.s. wavelength for SiO<sub>2</sub>-CdS composite materials prepared from TEOS and with different Cd<sup>2+</sup> mol % contents indicated in the Figure. The absorption spectra correspond to those of Fig 16b

A shoulder was observed for TMX samples which shifted from 460 nm to 408 nm. Table 18 shows the ranges of the shifted absorption band for different  $\text{Cd}^{2+}$  content. The measurements concerned about 15 samples for each composition.

A large blue shift towards 420 nm was observed in the absorption edge for lower  $\text{Cd}^{2+}$  content (TM15 samples). This can be associated with an intensification of the absorption edge (effective band gap) relative to the absorption at higher energy regions.

#### *6.3.2.1. Efros and Efros Model*

The Efros and Efros model is derived from the assumption of spherical particles surrounded by an infinitely high potential wall [13]. In our case, the previous results indicate that it is correct to apply it to our system which can be considered as consisting of discrete CdS particles (smaller than  $10^3$  nm) surrounded by amorphous silica which is a dielectric medium.

Size confinement occurs in the semiconductor sphere and the result is that the optical lines shift as a function of the sphere radii, as has been demonstrated on the absorption spectra. Thus the CdS quantum confinement will be strong for particle sizes smaller than 40 nm, medium when the size is less than 300 nm and finally particles with size greater than 1000 nm will present weak confinement effects.

Table 18

Shift range for gap energy of CdS nanoparticles with different  $\text{Cd}^{2+}$  mol % contents X for sono (TMX ) and classic (CTMX) host gels.

| Sample | Shift of<br>Absorption<br>band<br>(nm) |
|--------|--|
| TM40   | 460-435                                |
| TM30   | 450-427                                |
| TM15   | 444-420                                |
| CTM30  | 450-445                                |

According to this model the absorption edge is given by :

$$E = E_g + \frac{h^2}{8 \mu a^2}$$

where :

$h$  is the Planck's constant

$E$  , the absorption threshold

$E_g$  , the band gap of the bulk material

$\mu$  , the reduced mass between the electron and the hole

$a$  , the particle size radii

A linear behaviour of the exciton energy as a function of  $1/a^2$  is predicted. On this basis we have presented in Fig. 21 the exciton energy values obtained from the absorption spectra with the particle sizes averaged from the electron microscopy results. It shows that these experimental data can be fitted quite well by a straight line with 4.78 eV m<sup>2</sup> slope. From Efros and Efros equation this slope gives the effective reduced mass  $\mu$ . The calculated value from the Fig. 21 ,  $\mu=0.50$  , is three times greater than that corresponding to the bulk semiconductor. This ratio  $\mu_{\text{part.}}/\mu_{\text{bulk}} = 3$  has been also obtained by Nogami et al. [8] for CdSe particles in silica glasses.

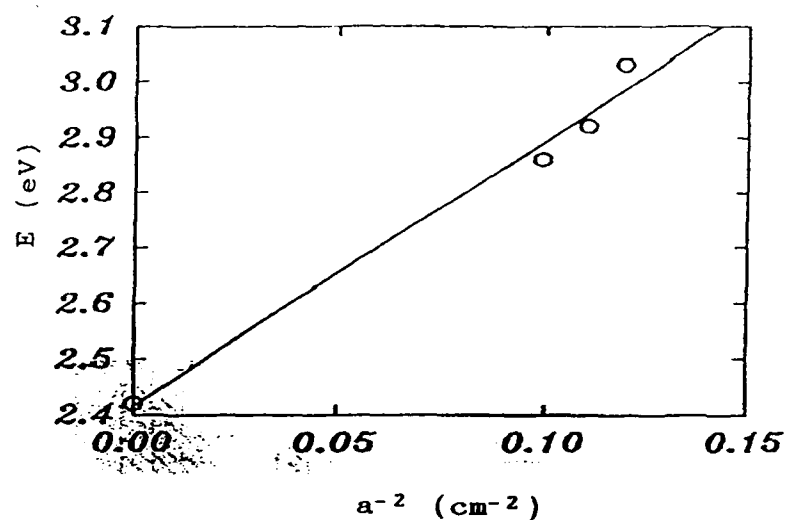


Figure 21. Plot of the exciton energy  $E$ , calculated from the absorption spectra as a function of the radius averaged from HRTEM photomicrographs. These experimental values fit quite well to the Efros and Efros model, indicated in continuous line.

## 7.FINAL EVALUATION OF RESULTS

### 7.1. Ceramic-Ceramic Composites

The experimental evaluation of the mechanical properties for ceramic-ceramic composites gave a higher fracture strength for hot-pressed samples than for conventionally sintered composites.

The matrix-fibre bonding obtained was found to be much better in the case of hot-pressed samples than for conventionally sintered composites. This was due to the glassy and fluid state of the matrix during hot-pressing. The best quality of the interfacial bond observed by SEM was presented for composites made from ceramic felts by infiltration process.

This means that the mechanical properties of ceramic-ceramic cordierite-based composites obtained by sonocatalytic approach were influenced by several parameters. The most important were the following :

- Densification methods (sintering ,hot-pressing or HIP) ,
- Reinforcing phases (short fibres or ceramic felts) ,
- Matrix structure (glass or crystalline)

The maximal flexural strength obtained for high temperature stabilized composites , at 1250 °C , was found to be equal to 139 MPa for a CT7fZ30 composite.



The overview of the mechanical characteristics of ceramic samples from sonogels shows that the flexure strength ranges between a minimum (55 MPa) for cordierite and a maximum (208 MPa) for cordierite-based ceramic composites .

The coefficients of thermal expansion obtained for different composites were of the same order as the theoretical value for the cordierite matrix ( $\approx 3.7 \cdot 10^{-6} \text{ }^{\circ}\text{C}^{-1}$  between 25  $^{\circ}\text{C}$  and 1000 $^{\circ}\text{C}$ ), and other values reported elsewhere for cordierite and cordierite-based composites.

It can be observed that the expansion coefficient decreased when the temperature of heat-treatment was increased from 900 $^{\circ}\text{C}$  to 1300 $^{\circ}\text{C}$ . This was attributed to the formation of  $\alpha$ -cordierite , the high-temperature stable form of the matrix.

Vickers' microhardness for these composites was higher than the average value reported for glass-ceramic materials , with  $H_v = 500$  to  $600 \text{ Kg mm}^{-2}$ . The experimental values obtained ranged between  $572 \text{ Kg mm}^{-2}$  for CT15A40 to  $961 \text{ Kg mm}^{-2}$  for CT157f30 .

That difference in  $H_v$  between composites obtained from fillers dispersion and composites prepared by infiltrating ceramic felts again shows the much greater quality of interfacial bond matrix-fibre for specimens made by infiltration of ceramic felts.

However , as indicated above , the resistance of these materials depended not only on the preparation method but on

the inherent characteristics of precursor materials. (e.g.  $\alpha$ -cordierite possesses a low fracture toughness, (1.75 MPa m<sup>1/2</sup> for cordierite sintered at 1300 °C, and 1.6 MPa m<sup>1/2</sup> for cordierite/ZrO<sub>2</sub> 50 % vol composite), which results in their low mechanical resistance ( $\approx$ 45 MPa).

In general the high mechanical strength of glass ceramics is attributed to their fine-grained microstructure, and the finer the grain size the higher the mechanical strength, the grain size depending on the heat-treatment schedule.

A more exhaustive control of sonochemistry and ceramic processing should lead to high performance materials with high mechanical strength.

It has been demonstrated that a very effective increase in the mechanical characteristics of the cordierite sonogel matrix can be easily obtained by infiltrating a ceramic felt.

This method seems potentially capable of developing higher strength by reinforcing a glass or ceramic matrix.

## 7.2. Inorganic Composites for Optical Applications

The selection of starting materials and conditions for preparing an optimal SiO<sub>2</sub> sonogel matrix where CdS nanoparticles can be formed at room temperature, was one of the more important aims of the present work.

The impregnation of CdS doped silica gels greatly improved the polishing treatment and strengthened the silica network.

The measurements of optical absorption spectra for these samples showed an important blue shift , up to 3.035 eV , in absorption band gap for TEOS-based with 5 % CdS non-impregnated samples.

The radii of CdS microcrystallites obtained from Efros and Efros' model were in the range of the experimental distribution of particle size established from HRTEM , which confirms the existence of quantum size effect.

## 8. FINAL CONCLUSIONS

1. The sonocatalytic approach for preparing mechanically resistant ceramic composites with a cordierite matrix has been revealed to be alternative way of procedure to that of conventional or classic sol-gel routes.
2. Ultrasonic radiation provides a control on gelation speed avoiding segregation of discontinuous short fibres.
3. Hot-pressing improves densification and hence the mechanical properties for composites.
4. Mechanical and thermal properties obtained from hot-pressed cordierite sonogels are comparable to those obtained from samples obtained by direct melting methods.
5. Optimization in mechanical resistance for cordierite from sonogels can be achieved by limiting to around 10 % wt., the concentration of  $\text{TiO}_2$  nucleant agent.
6. The interfacial bond between the matrix and the reinforcing phase can be optimized by infiltration of ceramic felts with the matrix- sonosol.
7. The flexural strength of the  $\text{ZrO}_2$  ceramic felt-reinforced cordierite matrix is higher than that of short fibre-reinforced cordierite composites. The former shows a zero porosity.

8. Sonogels with molar ratios of TMOS : water :  $\text{HNO}_3$  : FOR , which were respectively 1:10:0.45:3 , gave better texture and stability qualities , necessary for optical applications.

9. Impregnation of these gels substantially improved the physical and thermal stability and optical properties of CdS-doped gels.

10. Temperature of the method of preparation was lower than  $40^\circ\text{C}$ .

11. Particle size of CdS increased considerably from sono (5 nm) , to classic gels (25-50 nm)

12. An important blue-shift was observed for these sonogels which depended on  $\text{Cd}^{2+}$  concentration. The shift became largest (0.5 eV) when  $\text{Cd}^{2+}$  decreased to 5 % mol/mol  $\text{SiO}_2$

13. The use of ultrasonic irradiation in sol-gel techniques has been demonstrated to be very promising for preparing advanced ceramic-ceramic composite materials.

**BIBLIOGRAPHY.**

- [1]. N. de la ROSA FOX , L.ESQUIVIAS and J.ZARZYCKI , Rev. Phys. App. , 24 , Coll. C4-233 , (1989).
- [2]. M.ATIK , Thesis , Montpellier (1990).
- [3]. M.RAMIREZ , N. de la ROSA FOX , L.ESQUIVIAS and J.ZARZYCKI , J.Non-Cryst.Sol. , 121 , 84-89 , (1990).
- [4]. M.PIÑERO , M.ATIK and J.ZARZYCKI , J.Non-Cryst.Sol. , 147/8 , pp(--), (1992).
- [5]. N. de la ROSA FOX , L.ESQUIVIAS , A.CRAIEVICH and J.ZARZYCKI , J.Non-Cryst.Sol. , 121 , 211. (1990).
- [6]. B.W.DARWELL , J.Mat.Sci. , 25 , 757-780 , (1990)
- [7]. R.K.JAIN and R.C.LIND , J.Opt.Soc.Am. , 73 , 647 , (1982)
- [8]. M.NOGAMI , S.SUZUKI , AND K.NAGASAKA , J.Non-Cryst.Sol , 135 , 182-188 , (1991).
- [9]. Y.MAEDA , N.TSUKAMOTO , Y.YAZAWA , App.Phys.Lett. , 59 (24) , 3168-3170 , 1991.
- [10]. M.CANVA , P.GEORGES , A.BRUN , D.LARRUE , J.ZARZYCKI , J.Non-Cryst.Sol. , 141 , pp (--) , (1992).
- [11]. D.H.EVERETT , in "Characterization of Porous Solids " , Eds. S.J.Gregg , K.S.W.Sing and H.F.Stoeckli , p 253 , Soc.Chem.Ind. , London (19--)
- [12]. I.S.FEDOROVA and P.W.SCHMIDT , J.Appl.Cryst. , 11 , 405 , (1978).
- [13]. AI.L.EFROS and A.L.EFROS , Sov.Phys.Semicond. , 16(7) , 772-775 , (1982).